Botrytis cinerea strains infecting grapevine and tomato display contrasted repertoires of accessory chromosomes, transposons and small RNAs

Adeline Simon[1], Alex Mercier[1], Pierre Gladieux [2], Benoit Poinssot [3], Anne-Sophie Walker[1] and Muriel Viaud[1]*

[1] Université Paris-Saclay, INRAE, UR BIOGER, 78850 Thiverval-Grignon, France

[2] PHIM Plant Health Institute, Univ Montpellier, INRAE, CIRAD, Institut Agro, 34398 Montpellier, France

[3]Agroécologie, CNRS, INRAE, Institut Agro Dijon, Univ. Bourgogne, Université Bourgogne Franche-Comté, 21000 Dijon, France

[*] Corresponding author: muriel.viaud@inrae.fr

Abstract

The fungus *Botrytis cinerea* is a polyphagous pathogen that encompasses multiple host-specialized lineages. While several secreted proteins, secondary metabolites and retrotransposons-derived small RNAs have been characterized as virulence factors, their roles in host specialization remain unknown. The aim of this study was to identify the genomic correlates of host-specialization in populations of *B. cinerea* associated with grapevine and tomato. Using PacBio sequencing, we produced complete assemblies of the genomes of strains Sl3 and Vv3 that represent the French populations T and G1 of *B. cinerea*, specialized on tomato and grapevine, respectively. Both assemblies revealed 16 core chromosomes that were highly syntenic with chromosomes of the reference strain B05.10. The main sources of variation in gene content were the subtelomeric regions and the accessory chromosomes, especially the chromosome BCIN19 of Vv3 that was absent in Sl3 and B05.10. The repertoires and density of transposable elements were clearly different between the genomes of Sl3 and Vv3 with a larger number of subfamilies (26) and a greater genome coverage in Vv3 (7.7%) than in Sl3 (14 subfamilies, 4.5% coverage). An Helitron-like element was found in almost all subtelomeric regions of the Vv3 genome, in particular in the flanking regions of a highly duplicated gene encoding a Telomere-Linked Helicase, while both features were absent from the Sl3 and B05.10 genomes. Different retrotransposons in the Sl3 and the Vv3 strains resulted in the synthesis of distinct sets of small RNAs. Finally, extending the study to additional strains indicated that the accessory chromosome BCIN19 and the small RNAs producing retrotransposons Copia_4 and Gypsy_7 are common features of the G1 population that are scarcely if ever found in strains isolated from other populations. This research reveals that accessory chromosomes, repertoires of transposons and their derived small RNAs differ between populations of *B. cinerea* specialized on different hosts. The genomic data characterized in our study pave the way for further studies aiming at investigating the molecular mechanisms underpinning host specialization in a polyphagous pathogen.

Keywords: Fungi, PacBio genome sequence, secondary metabolism, helicase, Helitron, host specialization*, Vitis vinifera, Solanum lycopersicum*

28 **Introduction**

29

30 While specialist phytopathogenic fungi are highly specific to a single host plant, some other fungi stand
31 out for having a broad host range and are qualified as generalist. Nevertheless, these so-called
32 generalist pathogens could actually correspond to multiple co-existing populations that show a certain
33 level of host specialization (Gladieux et al., 2018; Stukenbrock & McDonald, 2008). Such scenario
34 provides an excellent opportunity to investigate the molecular determinants of host specialization. In
35 this regard, the grey mould fungus *Botrytis cinerea* has recently become a model of choice as both
36 powerful functional genomic tools and population data are available (Choquer et al., 2007; Mbengue
37 et al., 2016; van Kan et al., 2017; Veloso & van Kan, 2018). This ascomycete species is a necrotrophic
38 pathogen that infects more than 1400 host plant species belonging to 580 genera causing significant
39 damages in grapevine and in most cultivated fruits (Elad et al., 2015). Several studies conducted in
40 different parts of the world revealed that populations of *B. cinerea* are structured, and the host plant
41 was recognized as the factor with the highest explanatory power for this structure, ahead of geography
42 (reviewed in Walker, 2015). Notably French populations of *B. cinerea* isolated from tomato and
43 grapevine are differentiated from each other (Walker et al., 2015), and have higher aggressiveness on
44 their host-of-origin than other strains, indicating host specialization (Mercier et al., 2019). Recently,
45 Illumina sequencing of 32 representative isolates confirmed the subdivision of these *B. cinerea* French
46 populations into two genetic clusters on grapevine (G1 and G2 populations) and another, single cluster
47 on tomato that diverged from the G2 population (T population; Sup. Fig. S1; Mercier et al., 2021). These
48 genomic data also allowed to investigate the molecular differences underlying host specialization. By
49 characterizing single-nucleotide polymorphisms in Illumina short-read data, genes with footprints of
50 positive selection and/or divergent selection in the genomes of populations specialized to different
51 hosts were identified. These candidate genes that represent possible determinants of host
52 specialization were enriched in genes encoding Plant Cell Wall Degrading Enzymes (PCWDEs) and

53 transporters and in genes involved in the oxidative stress response. The same study also highlighted a
54 limited number of candidate genes that are population-specific including a couple of PCWDE-coding
55 genes and one secondary metabolism gene cluster (Mercier et al., 2021). Though this previous study
56 provided significant information about the evolution of *B. cinerea* genes in populations and identified
57 candidate genes possibly involved in host specialization, the lack of a complete assembly of the
58 sequenced genomes did not allow to investigate other mechanisms potentially involved in
59 specialization, such as (i) variation in the presence of accessory chromosomes, (ii) chromosomal
60 rearrangements, and (iii) differences in repertoires of transposable elements (TEs). This last point is of
61 particular interest since retrotransposons were shown to be the source of synthesis of small interfering
62 RNAs (siRNA) acting as effectors in *B. cinerea*. Indeed, these fungal siRNAs highjack the silencing
63 machinery of the plant cell to reduce the expression of genes involved in the defence process (Weiberg
64 et al., 2013; Porquier et al., 2021). High variability in the repertoire of TEs across fungal populations
65 and the fact that retrotransposons are the main source of siRNAs raise the possibility that these TEs
66 could be involved in host specialization.

67 In this study, our objective was to investigate whether strains from French populations of *B. cinerea*
68 specialized on tomato *versus* grapevine differ in genomic content in terms of core and accessory
69 chromosomes, TEs and small RNA repertoires. We characterized genome sequences produced with
70 the PacBio technology for two representative strains: the Sl3 strain that belongs to the T population
71 specialized on tomato and the Vv3 strain that belongs to the G1 population specialized on grapevine.
72 The full assembly of Sl3 and Vv3 genomes provided a complete view of the core and accessory
73 chromosomes as well as the full repertoires of genes and TEs. Small RNAs produced by the repertoires
74 of retrotransposons were also compared. Finally, extending the study to additional strains allowed to
75 identify which of the genomic features are associated to the populations specialized on tomato or
76 grapevine.

77

78 **Results**

79

80 **The genome architecture of the *Botrytis cinerea* strains Sl3 and Vv3 differ from the B05.10 strain in**
81 **their accessory chromosomes**

82 Genome assemblies based on PacBio Sequel sequencing data identified 16 core chromosomes (CCs)
83 and two accessory chromosomes (ACs) in both *Botrytis cinerea* strains Sl3 and Vv3 collected on tomato
84 and grapevine. Sequencing reads were assembled *de novo* using a combination of HGAP4 (SMRT-LINK
85 v5.0.1) (https://github.com/PacificBiosciences/) and CANU v1.6 (Koren et al., 2017). Both Sl3 and Vv3
86 assemblies consisted of 18 main contigs. The genome assemblies were estimated to be 43.2 Mb (Sl3)
87 and 44.9 Mb (Vv3), which is close to the 42.6Mb of the B05.10 genome (van Kan et al., 2017). Contigs
88 of the new genome assemblies were ordered and oriented as the previously described chromosomes
89 of B05.10 (BCIN01 to BCIN18) (Fig. 1), and then compared to the genome of B05.10 with QUAST
90 (Gurevich et al., 2013) (Sup. Table S1). The length (1.9-4.2 Mb) and GC content (41-43%) of the 16
91 largest contigs of Sl3 and Vv3 were similar to those of the 16 CCs defined in B05.10. In addition, the
92 high percentage of B05.10 genome coverage (94-99%) confirmed that the 16 largest newly sequenced
93 contigs corresponded to CCs BCIN01 to BCIN16 of *B. cinerea*. The length of CCs was homogenous across
94 the three strains, with less than 400 kb variation per CC (BCIN03: 3.6 Mb in Vv3, 3.3 Mb in Sl3 and 3.2
95 Mb in B05.10). The length (0.2-0.5 Mb) and GC content (<40%) of the two smallest contigs of Sl3 and
96 Vv3 was typical of ACs, as those found in B05.10. The percentage of B05.10 genome coverage indicated
97 that both strains had the AC BCIN17 (coverage >96%) while only Sl3 had an AC related to BCIN18 (52%
98 coverage). The second putative AC of Vv3 did not share any similarity with the genome of B05.10 and
99 corresponded to a new AC that we numbered BCIN19. Separation of chromosomes by pulse-field gel
100 electrophoresis confirmed the presence of two ACs in each strain (Sup. Fig. S2). According to the
101 migration, the two smallest chromosomes of the Sl3 strain had sizes that corresponded to the
102 assembled contigs BCIN17 and BCIN18 (299 and 188 kb). The same congruence was also observed for

103 the AC BCIN17 of the Vv3 strain (315 kb). In opposite, the migration of the second small chromosome
104 of Vv3, BCIN19 suggested that approximately 100 kb were missing in the corresponding contig (534
105 kb).

106 A criterion to evaluate the quality of a genome assembly is the presence of telomeres at the terminal
107 regions of the putative full chromosomes. For Sl3, telomeric repeats (*i.e*. TTAGGG repetitions; Levis et
108 al., 1997a) were found at both ends of eight chromosomes and at one end of eight other chromosomes
109 (Sup. Table S1). Only the assemblies of CCs BCIN1 and BCIN12 lacked both telomeric repeats. Thus,
110 telomeric repeats were missing at twelve chromosomal ends in the Sl3 assembly. In comparison,
111 telomeric repeats were missing at nine chromosomal ends in the B05.10 assembly (van Kan et al.,
112 2017), though not necessarily at the same chromosomal ends as in Sl3. Telomeric repeats in Vv3
113 contigs were retrieved only at the 5' end of CC BCIN2. To investigate the relative scarcity of telomeric
114 repeats in the Vv3 assembly, we searched the raw reads for telomeric repeats. We found 317 and 3712
115 occurrences of the telomeric repeat $(TTAGGG)_3$ and its reverse complement in Vv3 and Sl3 reads,
116 respectively. The relatively low abundance of telomeric repeats in sequencing reads of Vv3 indicated
117 that telomeric sequences were relatively rare in the library. This could be due to degradation of these
118 sequences during the preparation of libraries, as previously described (Tolios et al., 2015).

119 As the assemblies of the Vv3 and Sl3 genomes revealed different pairs of ACs, we further investigated
120 whether there was a correlation between the content in ACs and the host of origin. We used the 35
121 available genomic sequences of *B. cinerea* strains from three distinct populations specialized on
122 tomato (T population) or grape (G1 and G2 populations) as well as those of additional strains isolated
123 from bramble (Rf1, Rf2), hydrangea (Hm1), tomato (T4) and grapevine (BcDW1) (Mercier et al., 2021 ;
124 Amselem et al., 2011; Blanco-Ulate et al., 2013). Percentage of chromosome coverage showed
125 different distributions of the three ACs BCIN17, BCIN18 and BCIN19 (AC17 to 19; Table 1). The AC
126 BCIN17 first identified in B05.10 was detected in 30 other strains, including strains belonging to
127 populations T, G1 and G2 as well as in Rf1, Hm1 and BcDW1. The AC BCIN18 also identified in B05.10

128 was detected in seven other strains, including strains belonging to the T and G2 populations, Hm1 and
129 BcDW1. The AC BCIN19 identified in the Vv3 strain, was specific to the G1 group (detected in 11 strains
130 out of 12). Among populations T, G1 and G2, only G1 showed a relatively homogenous content in ACs
131 with the systematic presence of BCIN17, very high frequency of BCIN19 and absence of BCIN18.

132

133 **The core chromosomes of B05.10, Sl3 and Vv3 strains show a high level of synteny**

134 A vast majority of the genes identified in the reference strain B05.10 were retrieved in the Sl3 and Vv3
135 genomes. B05.10 gene annotation (van Kan et al., 2017) was transferred to Sl3 and Vv3 with the LIFTOFF
136 annotation mapping tool (Shumate & Salzberg, 2021). 11 661 and 11 609 genes were transferred to
137 Sl3 and Vv3 respectively, *i.e.* 99.6% and 99.2% of the 11 707 genes previously predicted in B05.10.
138 Altogether, 11 590 genes were retrieved in all three genomes, the vast majority in CCs (11 572 genes)
139 and very few in ACs (BCIN17: 18 genes). To assess synteny, we used SYNCHRO (Drillon et al., 2014), a
140 tool that reconstructs synteny blocks between pairwise comparisons of multiple genomes. As shown
141 in Sup. Fig. S3, the three sets of CCs were largely syntenic. When considering major synteny breaks, *i.e.*
142 those involving at least four adjacent genes that were not organized as in the B05.10 reference
143 genome, only one and two possible inversion events could be identified in Sl3 and Vv3, respectively
144 (Sup. Fig. S4). Two rearrangements between the terminal regions of chromosomes were also observed,
145 both accompanied by gene duplication. The first one involved a secondary metabolism gene cluster
146 with the polyketide synthase BcPKS7 as a key enzyme (Bcin10g00010-40). This cluster and the two 3'
147 flanking genes were located in two different regions in B05.10 and Vv3, *i.e.* the 5' end of BCIN10 in
148 B05.10 *versus* the 3' end of BCIN03 in Vv3. (Sup. Fig. S5). The rearrangement also resulted in the
149 duplication of a gene encoding a putative mitochondrial NADPH cytochrome b5 reductase in Vv3. The
150 second major subtelomeric rearrangement was observed when comparing the genomes of B05.10 and
151 Sl3. The nine first genes of BCIN08 in B05.10 (Bcin08g00010-90) were localized at the start of
152 chromosomes 2 and 15 in Sl3, while BCIN08 in Sl3 started with Bcin08g00080 (Sup. Fig. S6). Hence, the

153 genome of Sl3 contained two copies of seven of these genes and three copies of two of them. The
154 duplicated genes were predicted to encode a P450 monooxygenase, a laccase (*Bclcc11*), a glycoside
155 hydrolase possibly acting on hemicellulose or pectin chains (GH43 family; Lombard et al., 2014), a
156 glycosyl transferase, a heterokaryon incompatibility protein, a pyridine transferase as well as two
157 secreted proteins with unknown functions.

158

159 **Subtelomeric regions of core chromosomes and accessory chromosomes provide variation in gene**
160 **content**

161 The CCs of *B. cinerea* showed Presence Absence Variation (PAV) of genes in particular for secondary
162 metabolism gene clusters. To identify genes present in the Sl3 or Vv3 genomes but not in the B05.10
163 genome, we used the FGENESH *ab initio* gene-finder (Solovyev et al., 2006) and excluded the gene
164 models mapping in the B05.10 genome (Sup. Table S2). As shown in Fig. 1, *de novo* genes annotation
165 identified new genes in the CCs especially in their subtelomeric regions. When considering groups of
166 contiguous genes that were not shared between the three genomes, three secondary metabolism
167 gene clusters were identified based on the presence of genes encoding key enzymes. The first one was
168 only detected in Sl3 and included the gene encoding the previously identified SesquiTerpene Cyclase
169 BcSTC6 (BCIN_Sl3_03_394) (Amselem et al., 2011). The second gene cluster was identified in a
170 subtelomeric region of Vv3 and B05.10 (Bcin02g00013 to Bcin02g00016) and included a gene encoding
171 a non-ribosomal peptide synthetase-like similar to MelA , an enzyme involved in the biosynthesis of an
172 α-keto acid dimer in *Aspergillus terreus* (Geib et al., 2016). Finally, the third gene cluster was in a
173 subtelomeric region shared by Sl3 and Vv3 (BCIN_Sl3_10_11 to 26; BCIN_Vv3_10_2 to 14) and included
174 a gene predicted to encode a DiTerpene Synthase (DTC). When looking into previous Illumina
175 sequencing data (Mercier et al., 2021), these three secondary metabolism genes clusters had different
176 distributions: while the *Bcstc6* and the newly identified *Bcdtc* clusters were detected in strains of the

177 three different populations, the *BcmelA* cluster was present in all strains of the G1 and G2 groups but
178 absent from the T group (Table 1).

179 Fourteen subtelomeric genes coding for a protein predicted to be a helicase were identified in the
180 genome of Vv3 strain but not in the ones of B05.10 and Sl3 strains. This protein showed 51% similarity
181 with the Telomere-Linked Helicases (TLHs) identified in *Magnaporthe oryzae* (Gao et al., 2002;
182 Rehmeyer et al., 2009) and in *Ustilago maydis* (Sánchez-Alonso & Guzmán, 1998). It also shared the
183 same predicted domains *i.e.* two C2H2 zinc finger motifs, a helicase ATP-binding domain, a helicase C
184 domain and a specific TLH domain (Rehmeyer et al., 2009) ; Sup. Fig. S7). As in *M. oryzae* and *U. maydis*,
185 the 14 Vv3 helicase-encoding genes were localized in subtelomeric regions (11 regions). They were
186 located between 9 bp and 63 Kbp from chromosome ends, and six of them were actually the first genes
187 detected at the end of the chromosome. Incomplete copies of these helicase-encoding genes were
188 also detected in eight other subtelomeric regions (Sup. Fig. S8). Because of their homology with TLHs
189 of other fungi and of their genomic localization, these newly identified helicases were called BcTLHs.
190 PCR screening of *B. cinerea* populations further indicated that one or several copies of *Bctlh* are present
191 in a majority of strains specialized on grapevine, but also in few strains specialized on tomato or
192 isolated from other hosts (Table 1).

193 Accessory chromosomes were an additional source of PAV of genes among the B05.10, Sl3 and Vv3
194 strains (Fig. 1; Sup. Table S1). Firstly, the AC BCIN18 that was present in both Sl3 and B05.10 strains
195 was found to be only partially conserved as it carried seven genes that were shared between the two
196 strains, and nine contiguous genes that were present only in B05.10. Secondly, the newly identified AC
197 BCIN19 of the strain Vv3 carried 78 genes that were not present in the Sl3 and B05.10 strains. These
198 78 genes mostly encoded proteins with unknown functions, which is reminiscent of the gene content
199 of ACs BCIN17 and BCIN18 (van Kan et al., 2017). Nevertheless, a high proportion of the predicted
200 proteins displayed InterPro (IPR) domains that could be related to nucleic acids binding and

201 modifications (eight ribonucleases, two helicases, two zinc finger C2H2 proteins), transport through
202 vesicles (five dynamins) and peptidase activity (five peptidases) (Sup. Table S2).

203

204 **B05.10, Sl3 and Vv3 strains show different repertoires and densities of transposable elements**

205 Different subfamilies of Transposable Elements (TEs) were identified in the B05.10, Sl3 and Vv3 strains.
206 The complete annotation of TEs in the Sl3 and Vv3 genomes was carried out using a *de novo* approach
207 with the REPET package (Flutre et al., 2011; Amselem et al., 2015). Consensus sequences representing
208 all possible TEs among the Sl3 and Vv3 genomes were identified. After manual curation, 19 and 33
209 consensus TE sequences were retained for Sl3 and Vv3, respectively (Sup. File S1). They were classified
210 based on their structure and sequence similarities to characterized eukaryotic transposons (Hoede et
211 al., 2014; Wicker et al., 2007). Fifteen consensus sequences were previously identified in the B05.10
212 genome using the same pipeline and parameters as in the present study (Porquier et al., 2016).
213 Comparison of the B05.10, Sl3 and Vv3 consensus TE sequences revealed a total of 33 different
214 subfamilies: 13 class I LTR (retrotransposons), seven class II TIR (DNA transposons), one class II Helitron
215 and 12 subfamilies with either low genome coverage or vague classification (Fig. 2; Sup. Table S3). The
216 subfamily *Boty*/Gypsy_1 element (Diolez et al., 1995) was built from several *Boty* consensus as they
217 were identical in their central part and only differed at terminal regions (Sup. Fig. S9), as previously
218 observed in B05.10 (Porquier et al., 2016, 2021). In total, eight subfamilies were shared between the
219 three genomes, *i.e.* two subfamilies of Copia retrotransposons, four subfamilies of Gypsy
220 retrotransposons including the *Boty*/Gypsy_1 element and two subfamilies of the Tc1-Mariner DNA
221 transposons, including the *Flipper* element (Levis et al., 1997b). Fifteen, four, and three subfamilies
222 were exclusive to the Vv3, Sl3 or B05.10 genomes, respectively, and three subfamilies were shared
223 between two genomes. Libraries of subfamily sequences were used to annotate TE copies in the whole
224 genomes. For each subfamily, both full-length and truncated copies were retrieved in the genomes.

225 Genome coverage by subfamilies of TEs differed among the strains. Percentages of coverage for each
226 subfamily in each genome were computed (Fig. 2; Sup. Table S3). Total coverage by TEs was higher for
227 the Vv3 genome (7.7%), in which the largest number of subfamilies was identified, than in Sl3 and
228 B05.10 (4.5% and 3.7%, respectively) (Porquier et al., 2016). Transposable Elements were detected at
229 all chromosome ends but the 3' end of BCIN08 in Sl3 (Fig. 1), and also inside chromosomes, with a
230 significantly higher coverage in ACs (27.9-35.4%) than in CCs (1.9-11.3%). The eight shared subfamilies
231 were responsible for about 3% of the coverage in each genome whereas other subfamilies covered
232 approximately 1% of B05.10 or Sl3 genomes and 3.6% of Vv3 genome. The specific subfamilies
233 responsible for the higher coverage in Vv3 were mainly Copia and Gypsy retrotransposons and a TE
234 that was similar to a Helitron and covered 1.37% of the Vv3 genome.

235 The subtelomeric regions of the chromosomes of the Vv3 strain were invaded by a Helitron-like TE.
236 Helitron is a unique class of DNA transposons in eukaryotes and the representative elements of this
237 class encode a protein with two enzymatic domains corresponding to the helicase and the nuclease
238 activities that are required for transposition (Kojima, 2019). As only the helicase domain was clearly
239 identified in the TE found in Vv3, it was called a Helitron-like element (Sup. Fig. S10). Helitrons are also
240 known for their capacity to capture genes, which increases their size (Castanera et al., 2014). In
241 addition to a helicase-coding gene, the 15.5 kb sequence of the Helitron-like element found in Vv3
242 revealed two captured genes as well as relics of *Boty*/Gypsy_1 (*i.e.* Long Terminal Repeats). For one of
243 the captured genes, the predicted protein was a secreted pectate-lyase (IPR002022), similar to
244 enzymes involved in the maceration and soft rotting of plant tissue. Notably, 33 complete or
245 uncomplete copies of the Helitron-like TE carried this putative virulence gene in the genome of Vv3.
246 Unlike most TEs that were randomly distributed along chromosomes, the Helitron-like TEs were mainly
247 localized at the chromosome ends (Sup. Fig. S11). Looking closer at their precise localization, we
248 noticed that they were found in 3' and/or 5' of all the 14 complete copies of the helicase encoding
249 gene *Bctlh* (Sup. Fig. S8). Finally, to investigate how this Helitron-like TE was distributed among the
250 populations of *B. cinerea*, we designed PCR specific primers. The results indicated that all G1 strains

251 specialized on grapevine carried one or several copies of the Helitron-like TE while the element was
252 scarcely detected in the T population and detected in two strains out of four in the G2 population
253 (Table 1).

254 Fungi have developed defense mechanisms against invasion by TEs, including a Repeat-Induced Point
255 mutation (RIP) machinery that inactivates repeated sequences by causing Cytosine to Thymine
256 mutations and therefore decreases GC content. In a previous study, Amselem et al. (2015) showed that
257 the genome of *B. cinerea* contains the genes encoding the cytosine methyltransferases that are
258 required for RIP (BcRID1 and BcRID2), as well as TEs with signatures of RIP at both CpT (10-40% of TEs)
259 and CpA loci (10-35% of TEs). However, depending on the TE copy and on the *B. cinerea* strain, the
260 occurrence of RIP seems to be highly variable (Porquier et al., 2016, 2019, 2021). Regarding the
261 complete copies of TE from Sl3 and Vv3 (Fig. 3; Sup. Fig. S12) , the majority of the subfamilies displayed
262 copies with a large range of GC contents. For example, the Flipper DNA transposon showed both copies
263 with a GC content similar to those previously observed in a mobile copy (39%; Levis et al., 1997b) and
264 copies with a lower GC content (<20%) which could suggest inactivation by RIP. For each subfamily of
265 class I and II TEs identified in B05.10, copies with different GC content were observed. The same
266 pattern was observed for Sl3 except for subfamily Copia_2 for which all four copies had a GC content
267 > 40%. In contrast, the Vv3 genome included seven subfamilies of TEs, *i.e.* the Copia_2 and 4, Gypsy_5,
268 6 and 7, Mariner_4 and Helitron-like subfamilies, that contain only copies with GC content >40%
269 indicating the absence of RIP. Apart from Copia_2, these subfamilies are absent in the Sl3 and B05.10
270 genomes.

271

272 **Retrotransposons of the Sl3 and Vv3 strains produce different sets of small RNAs**

273 As retrotransposons and especially unripped copies are known to be the origin of the synthesis of small
274 RNAs in *B. cinerea* (Weiberg et al., 2013; Porquier et al., 2021), we investigated whether the different
275 repertoires of TEs in the Sl3 and Vv3 strains could lead to the production of different sets of small

276 RNAs. The two strains were grown both on grape and tomato juice solid media to partially mimic the
277 conditions that the fungus encounters on the host plants (Simon et al., 2013). The corresponding small
278 RNA libraries were Illumina-sequenced. After quality filtering (Sup. Table S4), only the reads between
279 20 and 24 nucleotides were kept as they correspond to the size of the small silencing RNAs generated
280 by the cleavage of long double stranded RNAs by the Dicer nuclease (Weiberg et al., 2013). A Principal
281 Component Analysis (PCA) of the repertoires of small RNAs in the four samples indicated that the two
282 strains harbour different repertoires, and that the use of grape *versus* tomato juice culture medium
283 had little impact on those repertoires (Sup. Fig. S13, A).

284 In order to identify which TEs were involved in the production of small RNAs, the reads from the Sl3
285 and Vv3 strains were mapped against the consensus sequences of the 33 identified TE subfamilies. The
286 results were similar with the two culture media and indicated that the TE-derived small RNAs were
287 produced by retrotransposons corresponding to seven subfamilies (Table 2, grey lines):

288 - Three out of six retrotransposons shared between Sl3 and Vv3 (*Boty*/Gypsy_1, Gypsy_3 and Gypsy_4)
289 produced small RNAs in both strains. These three retrotransposons were previously identified as the
290 only ones producing significant amounts of small RNAs in the B05.10 strain (Porquier et al., 2021).

291 - The unique retrotransposon found in Sl3 but not in Vv3 (Copia_6) produced small RNAs.

292 - Three out of six Vv3-specific retrotransposons found in Vv3 but not in Sl3 (Copia_4, Gypsy_6 and
293 Gypsy_7) produced small RNAs.

294 In addition to these qualitative differences, quantitative differences were also observed with Gypsy_3
295 producing the highest amount of small RNAs in the Sl3 strain (291.074 and 283.036 Reads Per Millions
296 (RPMs) in the grape and tomato juice media, respectively (Sup. Table S4) and Copia_4 producing the
297 highest amount of small RNAs in Vv3 strain (115.863 and 168.212 RPMs in the grape and tomato juice
298 media, respectively).

299 Sequences of the seven small RNA-producing TEs all showed the expected structure for Copia and
300 Gypsy classes of transposons (Wicker et al., 2007), except Gypsy_4 that lacked the GAG domain and
301 Copia_4 that had a small additional one (Sup. Fig S14). Small RNAs mapped almost all along the
302 sequences suggesting that the whole elements could be converted into small RNAs (except from the
303 GAG domain of Gypsy_3). All seven small RNA-producing TEs were in numerous complete copies (six
304 to 80; Sup. Fig. S12) all over the chromosomes of Vv3 or Sl3 strains. The three Vv3 specific small RNA-
305 producing TE, *i.e.* Copia_4, Gypsy_6 and 7, only showed copies with relatively high GC content (44.4%
306 +/-0.0, 47.4% +/-0.1 and 43.6% +/- 0.0 respectively). For the other small RNA-producing TEs, *i.e*
307 Gypsy_3, Gypsy_4, *Boty*/Gypsy_1 and Copia_6, copies with varied levels of GC were identified.
308 Nevertheless, mapping of the small RNA reads on the genomes showed that only copies with relatively
309 high GC content could generate small RNAs (Sup. Fig. S15).

310 Among *B. cinerea* small RNAs, the three siRNAs previously identified as effectors (*i.e.* siR5, siR3.1 and
311 siR3.2) were 21 bp in size and displayed the nucleotide U in first position (Weiberg et al., 2013). We
312 investigated which proportion of the small RNAs produced by the Vv3 and Sl3 strains shared the same
313 features (Sup. Fig. S16). For all seven TEs, the generated small RNAs were mainly composed of 22
314 nucleotide sequences (54-69%), followed by 21 nucleotide sequences (18-36%). Notably, a vast
315 majority of them (97%) showed an uracil (U) in first position. Finally, the three siRNA previously
316 identified as effectors in the strain B05.10 (*i.e.* siR5, siR3.1 and siR3.2) were identified among the four
317 libraries. Mapping data indicated that siR5 was produced by *Boty*/Gypsy_1 while siR3.1 and siR3.2
318 were produced by Gypsy_3, as previously demonstrated in the B05.10 strain (Weiberg et al., 2013;
319 Porquier et al., 2021).

320

321

322

323 **A set of retrotransposons-derived small RNAs is associated with the G1 population specialized on**
324 **grapevine**

325 As the repertoires of TE-derived small RNAs produced by the strains Vv3 and Sl3 were partially
326 different, we further investigated whether there was a correlation between the previously identified
327 populations of *B. cinerea* specialized on grapevine or on tomato (Mercier et al., 2021) and the
328 production of some of these small RNAs. The study was extended to a total of six strains from the T
329 population, four strains from the G1 population and three strains from the G2 population, as well as
330 to reference B05.10. All strains were grown on grape juice medium and small RNAs were investigated
331 as described above. Principal component analysis of small RNA repertoires (Sup. Fig. S13, B)
332 differentiated samples from the G1 population from samples from the G2 and T populations. To
333 compare the repertoires of TE-derived small RNAs from the 14 strains, we mapped the reads on the
334 TEs identified in B05.10, Sl3 and /or Vv3 strains (Table 2; Sup. Table S4). Mapping data indicated that
335 the same seven retrotransposons that produced small RNAs in B05.10, Sl3 or Vv3 strains could be
336 responsible for the production of small RNAs in the other tested strains. An exception was observed
337 for the Vv9 strain as its small RNAs did not map to any of the known TEs. It should be noted here that
338 for Vv9 and the other ten strains where only unassembled genome sequences are available (Illumina
339 data), additional unknown retrotransposons may be involved in the production of small RNAs. From
340 the presented analysis, the following distribution of retrotransposons derived-small RNAs in the
341 different populations could be observed:

342 - Small RNAs produced by the shared *Boty*/Gypsy_1 and Gypsy_4 TEs were identified in most of the
343 strains from the three populations and in the strain B05.10.

344 - Small RNAs produced by the shared Gypsy_3 TE were identified in most of the strains of the T and G1
345 populations and in the strain B05.10, but not in three strains of the G2 population.

346 - Small RNAs produced by the Sl3-identified Copia_6 TE were only identified in Sl3 and another strain
347 of the T population (Sl6).

348 - Small RNAs produced by the Vv3-identified Copia_4, Gypsy_6 and Gypsy_7 TEs were exclusively
349 identified in G1 strains. This could explain why the G1 strains separated from the other strains in the
350 PCA analysis (Sup. Fig. S13, B). In the genome of Vv3, Copia_4, Gypsy_6 and Gypsy_7 were detected in
351 10, 12 and 23 complete copies, respectively (Sup. Fig. S12). Copia_4 was localized on several CCs, while
352 Gypsy_6 and Gypsy-7 were found both on CCs and ACs (Sup. Fig. S17). The G1-specific AC BCIN19
353 revealed seven complete copies of Gypsy_7.

354 We further focused on the potential G1-specific small RNAs by investigating the presence of the three
355 corresponding retrotransposons in strains from the T, G1 and G2 populations and strains from other
356 hosts. Copia_4, Gypsy_6 and Gypsy_7 were searched by PCR using one pair of specific PCR primers per
357 TE. These primers were defined in conserved regions of TEs and were expected to amplify at least the
358 unripped copies of TEs containing these regions (Sup. Fig. S18). As shown in Table 1, Copia_4 was
359 detected in all the G1 strains tested (12 strains) but not in the T and G2 populations (13 and 4 tested
360 strains, respectively). Gypsy_7 was detected in all strains of the G1 population but one (Vv2), in one
361 strain of the G2 population (Vv8) but not in the T population. Finally, Gypsy_6 was detected in only
362 three strains of the G1 population (Vv3, Vv10 and Vv13). Unexpectedly, the PCR approach did not allow
363 to detect Gypsy_6 in Vv1, Vv5 and Vv14 strains, whereas small RNAs generated from this TE were
364 isolated from the same strains (Table 2). We therefore investigated the mapping of these small RNAs
365 on the Gypsy_6 TE identified in the Vv3 strain (Sup. Fig. S18, C). For Vv5, no small RNA read mapped
366 on the loci of the PCR primers allowing for the possibility that these regions were not conserved in Vv5.
367 By contrast, some small RNAs generated by the Vv1 and Vv14 strains mapped to the Gypsy_6 regions
368 where the PCR primers were defined. One remaining hypothesis to explain the absence of PCR product
369 could be the absence of a copy of Gypsy_6 containing both primer regions in Vv1 and Vv4 genomes. In
370 conclusion, while the absence of PCR products should be interpreted with caution, the results indicated
371 that the small RNA generating-TE Copia_4, and to a lesser extent, Gypsy_7, are enriched in the G1
372 population.

373 **Discussion**

374

375 While the genomes of several strains of the polyphagous pathogen *B. cinerea* have already been
376 sequenced allowing studies of genetic variation (Atwell et al., 2015; Mercier et al., 2021), only one
377 gapless genome, whose of the model strain B05.10, was available so far (van Kan et al., 2017). In this
378 study, we used the PacBio technology to sequence the full genomes of the Sl3 and Vv3 strains that
379 represent two populations of *B. cinerea* specialized to tomato (T population) and grapevine (G1
380 population; Mercier et al., 2021). We also used additional strains of these two populations and strains
381 from a second population specialized to grapevine (G2) to extend our comparative analyses to a larger
382 set of pathogens.

383

384 **The full genomic assemblies of *B. cinerea* strains from different populations reveal highly syntenic**
385 **core chromosomes**

386 The long-reads generated with the PacBio technology allowed us to generate genome assemblies of
387 43.2 Mb and 44.9 Mb, for the strains Sl3 and Vv3, respectively. These assembly lengths are close to
388 that of the reference strain B05.10 (42.6 Mb). Additionally, almost all genes (>99%) previously
389 annotated in the strain B05.10 were identified in the generated assemblies. As shown by sequence
390 comparison and gene annotation, the three strains share 16 CCs with a high level of synteny with only
391 few events of inversions or translocations. The same number of CCs was also observed in the other
392 genomes of *Botrytis* and Sclerotiniaceae species (Derbyshire et al., 2017; Valero-Jiménez et al., 2020).
393 The high level of synteny between the CCs of *B. cinerea* strains is consistent with their interfertility, as
394 synteny is needed for appropriate chromosome pairing during meiosis. Direct evidence for interfertility
395 comes from a fertile progeny that was obtained by crossing Sl3 and Vv3 (M. Viaud, *unpublished data*).

396 Indirect evidence for interfertility can be found in population genetic analyses, which previously
397 indicated gene flow between the T and G1 groups to which Sl3 and Vv3 belong (Mercier et al., 2021).

398

399 **The accessory chromosomes BCIN19 is specific to the *B. cinerea* G1 population specialized on**
400 **grapevine**

401 The full genomic assemblies generated in this study revealed that Sl3 and Vv3 strains have different
402 pairs of ACs characterized by their small sizes (0.2-0.6 Mbp), their low GC content (25-38%) and a high
403 density of TEs (28-35%). While the Sl3 strain carries two ACs similar to those of B05.10 (BCIN17 and
404 BCIN18), the Vv3 strain carries BCIN17 and a newly characterized AC named BCIN19. Extending our
405 study to 35 *B. cinerea* strains confirmed the dispensability of BCIN17, BCIN18 and BCIN19 and did not
406 support any lineage specificity for BCIN17 and BCIN18. In opposite, our data suggest that BCIN19 is
407 specific to the G1 group specialized on grapevine. Exploring further the distribution and conservation
408 of the ACs in larger samples would allow to define more precisely to which extent some parts of the
409 accessory genome are associated with a specific population. Though the function of fungal ACs remains
410 largely elusive, several studies on phytopathogenic species reported that ACs could carry genes
411 encoding effectors or genes involved in the synthesis of toxic metabolites (Bertazzoni et al., 2018;
412 Meena et al., 2017; Yang et al., 2020). Our study indicates that ACs are an important source of variation
413 in gene content in *B. cinerea*, but at this stage, none of the 78 genes carried by the ACs has a predicted
414 function indicating a direct role in pathogenicity. Accessory chromosomes could also be considered as
415 reservoirs of TEs. Interestingly, BCIN19 carries several copies of the Gypsy_7 retrotransposon that is
416 specific of the G1 population and generates small RNAs.

417

418

419 **The genome of the *B. cinerea* strain Vv3 has a larger repertoire of transposable elements than the**
420 **Sl3 and B05.10 strains**

421 Transposons are important features of fungal genomes playing key roles in genome structure, genome
422 plasticity (Fouché et al., 2021), and production of small RNAs (Weiberg et al., 2013). TEs identified in
423 the three fully sequenced and assembled genomes of *B. cinerea* strains B05.10, Sl3 and Vv3 cover 3.7,
424 4.5 and 7.7% of their genomic sequences, respectively. Variation in TE content explains most of the
425 variation in total assembly length, with the genomic sequences varying between 41.0 and 41.4 Mb
426 when TEs are excluded. As already observed in the B05.10 strain (van Kan et al., 2017), TEs identified
427 in the Sl3 and Vv3 strains are frequent in the subtelomeric regions of the CCs, as well as in ACs where
428 they can cover up to one third of the sequence. While previous studies already indicated variation in
429 the presence of TEs (e.g *Boty* and *Flipper*) in *B. cinerea* strains (Amselem et al., 2011; Porquier et al.,
430 2021), our study is the first that compares TEs between fully assembled genomes. Our data clearly
431 show that the repertoires of TEs are very different between the three sequenced strains and 21 new
432 subfamilies of TEs were recovered, mostly from the Vv3 strain. As in many fungi, TEs of *B. cinerea* could
433 be inactivated by RIP (Amselem et al., 2015; Porquier et al., 2016, 2019, 2021). In our analysis, the GC
434 content of TE copies suggests that RIP is less active in the Vv3 strain, consistent with its larger TE
435 content. This larger content is due to retrotransposons, TIR transposons, as well as to a Helitron-like
436 TE. Several subfamilies of the TEs identified in this strain, including retrotransposons and the Helitron-
437 like TE, do not show any traces of RIP and could possibly be able to transpose in new *loci.*

438

439 **Rearrangements at chromosome ends are a source of gene gains and losses in *B. cinerea***

440 Our synteny and PAV analyses indicate that the few rearrangements occurring in the CCs correspond
441 mainly to exchanges of chromosomes ends, and that most gene gains or losses also happen in these
442 TE-rich regions. In many fungi, subtelomeric regions are enriched in secondary metabolism gene
443 clusters (Kjærbølling et al., 2020). Therefore, rearrangements in these regions could contribute to the

444 intraspecific diversity of the biosynthetic clusters (Olarte et al., 2019). In the genome of *B. cinerea*, six
445 out of the approximately 40 identified secondary metabolism gene clusters are in subtelomeric regions
446 (Amselem et al., 2011; van Kan et al., 2017). The present study provides evidence that the evolution of
447 some of these subtelomeric clusters is subjected to chromosomal ends exchange (PKS7 cluster) as well
448 as to gene gains and losses (MelA-like and DTC clusters). In other studies, partial or total loss of the
449 subtelomeric gene cluster responsible for the biosynthesis of the botcinic acid phytotoxin was
450 observed in some rare strains of *B. cinerea* and in other species of *Botrytis* (Plesken et al., 2021; Valero-
451 Jiménez et al., 2020).

452 In addition to gene gains and losses, our study revealed that duplication of *B. cinerea* genes occurs in
453 subtelomeric regions. For example, the four colocalized genes (Bcin08g00060 to 90) possibly related
454 to detoxification of reactive oxygen species or plant cell wall degradation and previously identified as
455 duplicated in strains specialized to tomato (T group; Mercier et al., 2021) were localized on two
456 different chromosomes ends of the Sl3 strain.

457 Subtelomeric regions of all three B05.10, Sl3 and Vv3 strains were found to be enriched in TEs, and TEs
458 were detected in the exchanged chromosomal ends mentioned above. Similar observations made in
459 other fungal genomes led to the hypothesis that TEs may be responsible for repeat-driven
460 recombination and gene rearrangements (Fouché et al., 2021; Lind et al., 2017; Olarte et al., 2019). If
461 these exchanges of chromosomes ends are later followed by a sexual cycle in which chromosome
462 pairing occurs between CCs that have different extremities, it could result in gene gain or loss. Indeed,
463 in this scenario, the progeny would include individuals with two copies of one initial subtelomeric
464 region or none of them. This two-steps mechanism could have an important role in the evolution of
465 the repertoire of secondary metabolites produced by *B. cinerea.*

466

467

468 **A helicase encoding gene and a Helitron-like element shape the subtelomeric regions of the genome**
469 **of the *B. cinerea* strain Vv3**

470 Analysis of the genome of the *B. cinerea* strain Vv3 revealed that subtelomeric regions show a
471 particular structure with the co-occurrence of a Telomere-Linked Helicase (TLH) encoding gene and a
472 Helitron-like TE that were not described so far in this species. Genes encoding TLHs were previously
473 described in the subtelomeric regions of the fungal pathogens *M. oryzae* and in *U. maydis* (Gao et al.,
474 2002; Rehmeyer et al., 2009; Sánchez-Alonso & Guzmán, 1998). The Vv3 genome contains 14 copies
475 of the *Bctlh* gene, all in subtelomeric regions and, strikingly, all flanked in 3' and/or 5' by a copy of a
476 Helitron-like TE. Helitrons were described in other fungi *i.e. Pleurotus ostreatus* and *Fusarium*
477 *oxysporum* (Castanera et al., 2014; Chellapan et al., 2016) but, to our knowledge, this is the first study
478 that shows a strong enrichment of this family of TEs in subtelomeric regions. One hypothesis to explain
479 the localization of the Helitron-like TE of *B. cinerea* could be that it preferentially inserts in the flanking
480 regions of the *Bctlh* gene copies. Nevertheless, as no nuclease domain was detected in the sequence
481 of Helitron-like TE, this may question its ability to transpose (Kojima, 2019). Alternatively, the
482 occurrence of the *Bcthl* gene and Helitron-like TE in the subtelomeric regions could arise from
483 recombination between chromosome ends followed by sexual crosses leading to duplications as
484 discussed above. Indeed, when these mechanisms are repeated in successive generations, they could
485 lead to the homogenization of the subtelomeric regions. Previous studies revealed a drastic reduction
486 of the number of Restriction Fragment Length Polymorphisms (RFLPs) in subtelomeric regions of *B.*
487 *cinerea* strains isolated from grapevine suggesting a possible homogenization of these regions (Levis
488 et al., 1997a). Based on our analysis, one may wonder whether this homogenization is due to the
489 amplification of the *Bcthl* genes and Helitron-like TEs by exchanges and duplications of chromosomes
490 ends.

491 Another original feature of the 15.5 kb sequence of the Vv3 Helitron-like TE is that it carries captured
492 genes, as in some other Helitrons elements (Castanera et al., 2014). It would be interesting to evaluate

493 the expression of these captured genes especially the one encoding a putative secreted pectate-lyase
494 and to test whether the numerous copies (33) present in the Vv3 genome confer a higher ability to
495 degrade host tissues. Our analysis to *B. cinerea* populations indicated that the Helitron-like TE is
496 present in all the strains of the G1 group, in about half of the strains of the G2 group and in a minority
497 of strains of the T group which further questions its potential role in the interaction with the host plant.

498

499 **Both Gypsy and Copia retrotransposons generates small RNAs in *B. cinerea***

500 *Botrytis cinerea* produces siRNA that are acting as effectors in the host plant where they can highjack
501 the silencing machinery to impair the expression of genes involved in the defence process (Weiberg et
502 al., 2013). As in other fungal models, these small RNAs are mainly synthesized from retrotransposons.
503 The work just published by Porquier et al., (2021) actually identified *Boty*/Gypsy_1, Gypsy_3 and
504 Gypsy_4 as the only TE producing small RNAs in B05.10, and the authors demonstrated that the
505 Gypsy_3 TE could be considered as a pathogenicity factor by itself as the introduction of Gypsy_3 in a
506 strain lacking this TE resulted in the production of siRNA and an enhanced aggressiveness on tomato
507 and on *Arabidopsis thaliana*. In our study, we demonstrated that the Sl3 and Vv3 strains that have very
508 different repertoires of TEs are consequently able to produce different sets of TE-derived small RNAs.
509 Seven retrotransposons, five Gypsy subfamilies but also two Copia subfamilies, were identified as
510 responsible for their production. A common feature of all the copies of TEs that generate small RNAs
511 in the Vv3 and Sl3 strains is that they show a relatively high GC content. By contrast, the AT-rich copies
512 of the same subfamilies do not produce small RNAs. These data corroborate those of Porquier et al.
513 (2021), who observed that the production of small RNAs in the B05.10 strain correlates positively with
514 the retrotransposon GC content and negatively with a RIP index. This suggests that only
515 retrotransposons that are not inactivated by RIP are able to be expressed and therefore to generate
516 small RNAs. Furthermore, the small RNAs generated by the seven retrotransposons present in Sl3
517 and/or Vv3 strains all show the same features, *i.e.* a size of 21-22 nucleotides and a preference for a 5'

518 terminal U. These features are believed to be required to associate with the plant AGO1 and activate
519 the gene silencing process (Weiberg et al., 2013).

520 Among the seven small RNA generating-retrotransposons that were identified, three Gypsy subfamilies
521 *i.e*. *Boty*/Gypsy_1, Gypsy_3 and Gypsy_4 are present in both Vv3 and Sl3 strains as well as in B05.10
522 (Porquier et al., 2021) and are responsible for the synthesis of a common set of small RNAs that
523 includes the characterized effectors siR5, siR3.1 and siR3.2 (Weiberg et al., 2013). In addition to the
524 shared repertoire of small RNAs mentioned above, the Vv3 and Sl3 strains produce additional small
525 RNAs through the Copia_4, Gypsy_6, Gypsy_7 (Vv3) and Copia_6 (Sl3) retrotransposons. These newly
526 characterized TEs and the small RNAs that they generate therefore confirm that the difference in the
527 repertoires of retrotransposons present in *B. cinerea* strains Sl3 and Vv3 has strong impact on the
528 production of potential small RNA effectors.

529

530 **The *B. cinerea* G1 population specialized on grapevine produces a specific set of small RNAs**

531 Investigating the repertoires of small RNAs and the presence of some of the small RNA-producing TEs
532 in a larger set of strains *B. cinerea* highlighted some significative differences between the three
533 considered populations. While some sets of TE-derived small RNAs are present in strains belonging to
534 different populations, some seem to be specific to one genetic group. Small RNAs produced by
535 *Boty*/Gypsy_1, Gypsy_3 and Gypsy_4 are not only produced by the B05.10, Sl3 and Vv3 strains but
536 appear to be commonly produced in the T and G1 populations which could suggest that this set plays
537 a conserved role that is important in the interaction with different hosts. This is indeed the case for
538 the characterized Gypsy_3-derived siRNAs that were shown to silence genes both in *Arabidopsis*
539 *thaliana* and in tomato (Weiberg et al., 2013 ; Porquier et al., 2021). Regarding the three analyzed
540 strains of the G2 population, only *Boty*/Gypsy_1- and Gypsy_4-derived small RNAs could be identified
541 but uncharacterized TEs may generate other small RNAs. A full assembly of the genome of one the G2
542 strains would be required to answer this question.

543 Finally, our data revealed that two retrotransposons, Copia_4, and to a lesser extent Gypsy_7, occur
544 at high frequency in the G1 population where they jointly generate an important proportion of the
545 arsenal of TE-derived small RNAs. The genome of the Vv3 strain harbors ten complete copies of
546 Copia_4 on CCs, and 23 complete copies of Gypsy_7 shared between the CCs and the AC BCIN19 that
547 is specific to the G1 population. By contrast, these two TEs were very rarely detected by PCR in other
548 strains of the T and G2 populations (this study) and they were not either retrieved in the genomic
549 sequences of *B. cinerea* strains B05.10 (van Kan et al., 2017), T4 (Amselem et al., 2011) and BcDW1
550 (Blanco-Ulate et al., 2013). Using a larger number of strains from the G1 and G2 populations as well as
551 strains from other hosts would be valuable to investigate further the distribution of these sources of
552 small RNAs. If they are confirmed to be mainly present in the G1 population specialized on grapevine,
553 it will be tempting to hypothesize that they have been maintained because they have a significant role
554 in this interaction, either directly with the host *i.e.* through the silencing of grapevine genes, either
555 indirectly *e.g.* by acting on other microorganisms present in the same ecological niche. Nevertheless,
556 the fact that the G2 strains do not have the Copia_4 and Gypsy_7 TEs suggests that their potential role
557 is not needed in all *B. cinerea* populations found on grapevine. Functional studies will be required to
558 answer these questions.

559

560 **Conclusion**

561 Our study was conducted in order to investigate the genomic determinants of host specialization in *B.*
562 *cinerea.* Previous work revealed widespread signatures of positive selection in the T population
563 specialized to tomato, with genes under positive selection encoding cellulases, pectinases and
564 enzymes involved in the oxidative stress response suggesting that these activities may contribute to
565 the specialization on tomato (Mercier et al., 2021). The present study substantially extends these
566 findings by revealing that populations of *B. cinerea* specialized on different hosts harbor different sets
567 of accessory chromosomes, repertoires of transposons and their derived small RNAs. Hence, we

568 identified genomic features that are specific to the main population specialized to grapevine in France
569 (the G1 population). The retrotransposons Copia_4 and Gypsy_7 allow the production of a G1-specific
570 set of small RNAs with structures similar to the known effector siRNA (Weiberg et al., 2013). In
571 addition, strains of the G1 population specifically carry the newly characterized BCIN19 accessory
572 chromosome that includes several copies of the Gypsy_7 elements and newly identified genes whose
573 functions remained to be characterized. Our characterization and analysis of new genomic data in
574 populations of *Botrytis* specialized to different hosts pave the way for new molecular investigations of
575 the mechanisms underlying host specialization in this polyphagous pathogen.

576

577

578 **Methods**

579 **Genome sequencing and assembly**

580 The *Botrytis cinerea* Sl3 and Vv3 strains were isolated from the Champagne region (France) respectively
581 from tomato (cultivar Moneymaker) and grapevine berries (Pinot noir), as previously described
582 (Mercier et al., 2021). For DNA sequencing, these strains were cultivated three days in liquid malt
583 medium. High-molecular-weight DNA was extracted using a sarkosyl procedure in which the ethanol-
584 precipitated DNA was fished with a glass hook to avoid centrifugation and DNA breaks. Sl3 and Vv3
585 genomic DNA were sequenced using a PacBio Sequel sequencer (KeyGene, Wageningen, NL). Total
586 lengths of respectively 8.3Gb and 4.7Gb reads were obtained with mean lengths of 8.4Kb and 11.3Kb.
587 The theorical coverages of the genome were thus of 195X and 120X. Reads were assembled with
588 HGAP4 (SMRT-LINK v5.0.1) (https://github.com/PacificBiosciences/) and CANU v1.6 (Koren et al., 2017).
589 HGAP4 was run with the set of parameters recommended for fungal genomes (https://pb-
590 falcon.readthedocs.io/en/latest/parameters.html). CANU was run with default parameters and an
591 expected coverage of 42Mb. HGAP assemblies were polished with pilon (Walker et al., 2014) using Sl3
592 or Vv3 Illumina reads (Mercier et al., 2021). CANU assemblies were polished with both arrow
593 (https://github.com/PacificBiosciences/) and PILON. Mitochondrial, ribosomal and small redundant
594 contigs were removed, and final versions of assemblies were manually compiled from polished runs of
595 HGAP and CANU assemblies. Both genome assemblies were evaluated and compared with B05.10
596 referent genome (van Kan et al., 2017) using QUAST (Gurevich et al., 2013). For the separation of ACs
597 by gel electrophoresis, chromosomal DNA was prepared as described by van Kan et al. (1993) and
598 loaded on a 1% agarose gel (SeaKem Le, FMC) in 0.5X Tris Borate EDTA buffer. Chromosomes were
599 then separated using a Contour-clamped Homogeneous Electric Field (CHEF) apparatus (DRIII, BioRad)
600 using the following parameter: 6 V/cm; 120° angle; 50-90 seconds switch; 22 hours; 14°C.

601

602

603 **Transposable elements prediction**

604 Transposable elements (TEs) were annotated using the REPET package
605 (https://urgi.versailles.inra.fr/Tools/REPET ; (Amselem et al., 2015) as previously described in Porquier
606 et al., 2016 for the genome of the *B. cinerea* reference strain B05.10. Briefly, the TEDENOVO pipeline
607 (Flutre et al., 2011) was used to detect repeated elements in the genome and to provide a consensus
608 sequence for each family. Consensus sequences were then classified using the PASTEC tool (Hoede et
609 al., 2014), based on the Wicker hierarchical TE classification system (Wicker et al., 2007). After manual
610 correction, the resulting library of consensus sequences was used to annotate TE copies in the whole
611 genome using the TEANNOT pipeline (Quesneville et al., 2005). Consensus sequences identified from
612 different genomes were compared and considered as the same subfamily based on a bidirectional best
613 hit approach (blastn with evalue < 1e-10 and coverage > 70%). Presence of the subfamilies in the
614 genomes of additional strains (Table 1) was tested by PCR using the MyTaq polymerase (Bioline) and
615 the primers listed in Sup. Table S5.

616

617 **Gene prediction, synteny**

618 The structural annotation of B05.10 genes (van Kan et al., 2017)
619 (http://fungi.ensembl.org/Botrytis_cinerea/) was transferred to Vv3 and Sl3 genomes using the LIFTOFF
620 annotation mapping tool (Shumate & Salzberg, 2021). Genes were also predicted *de novo* using the
621 FGENESH *ab initio* gene-finder (Solovyev et al., 2006) (http://www.softberry.com/berry.phtml) with the
622 *Botrytis* matrix. Presence/absence of genes in other genomes was determined with blastn analyses.
623 The synteny between B05.10, Sl3 and Vv3 genes was analysed with SYNCHRO (Drillon et al., 2014), which
624 detects ortholog proteins with Reciprocal Best Hit (RBH). SYNCHRO was run with a best score threshold
625 (min_sim_RBH) of 80, a length ratio threshold (max_diflen) of 1.3 and a delta value of 3 (medium
626 stringency). Duplications of gene clusters were further explored with CLINKER (Gilchrist & Chooi, 2021).

627 Presence of the gene *Bctlh* in the genomes of additional strains (Table 1) was tested by PCR using the
628 MyTaq polymerase and the primers indicated in Sup. Table S5.

629

630 **Small RNA sequencing and analysis**

631 *Botrytis cinerea* strains were cultivated 48 hours on solid media made from grape juice or tomato juice
632 supplemented with agar and covered with a sheet of cellophane as previously described (Simon et al.,
633 2013). RNAs were extracted with the TRIzol reagent (InvitroGen) and submitted to a DNAse treatment
634 (DNA-free kit, Ambion). Total RNAs were purified with miRNeasy kit (Qiagen) which allows the
635 selection of the RNA fraction less than 100 bases. Small RNA libraries were prepared and sequenced
636 at Integragen (https://www.integragen.com/). Libraries were generated following (Vigneault et al.,
637 2012), with adjustments to improve ligation, from at least 1 µg of extracted total RNA with a RIN
638 greater than 7. Libraries were sequenced on Illumina HiSeq4000. Quality of raw sequence data was
639 checked with FASTQC (https://www.bioinformatics.babraham.ac.uk/projects/fastqc/). After removal
640 of adapters with CUTADAPT (Martin, 2011), reads shorter than 16 bases were discarded. Reads were
641 then processed using FASTX-TOOLKIT (http://hannonlab.cshl.edu/fastx_toolkit/) as in Weiberg et al.
642 (2013), *i.e.* low-quality sequences were filtered out with FASTQ_QUALITY_FILTER -q 30 -p 70, low-
643 complexity sequences were filtered out with FASTX_ARTIFACTS_FILTER, and finally identical sequences
644 were counted with FASTX_COLLAPSER. Only sequences 20-24 nucleotides length and with more than five
645 reads per million in at least one library were kept for further analyses. Principal Component Analyses
646 (PCA) were performed to visualize the distance between samples. Reads were mapped against B05.10
647 (van Kan et al., 2017), Sl3 and Vv3 genomes, against TE consensus and against TE complete copies in
648 the three genomes with the GLINT software (https://forge-dga.jouy.inra.fr/projects/glint/wiki); only
649 perfect matches (100% identity and 100% coverage) were considered. As a control, unprocessed (raw)
650 reads were mapped the same way to verify that no additional small RNA-producing TE could be
651 identified.

652 **Acknowledgements**

653 We are grateful to the following bioinformatics platforms and partners for providing computational
654 support and/or storage resources : Bioinfo Genotoul,
655 (https://doi.org/10.15454/1.5572369328961167E12), CATI BARIC (https://www.cesgo.org/catibaric/),
656 INRAE-URGI, INRAE-LIPME Bioinfo (Jérôme Gouzy, Sébastien Carrère, Erika Sallet) and INRAE-BIOGER
657 Bioinfo (https://bioinfo.bioger.inrae.fr/ ; Nicolas Lapalu). We thank Alexander H. J. Wittenberg
658 (KeyGene, Wageningen, NL) and Jean-Paul Saraiva (Integragen, Evry, France) for the PacBio and
659 Illumina sequencing, respectively.

660

661 **Funding**

662 This work was supported by a grant overseen by the French National Research Agency (ANR) as part
663 of the "Investissements d'Avenir" (LabEx BASC; ANR-11-LABX-0034) and "Priority Research" programs
664 (PPR VITAE; ANR-20-PCPA-0010) and by the INRAE department SPE. The BIOGER unit also benefits from
665 the support of "Saclay Plant Science-SPS" (ANR-17-EUR-0007). AM was supported by a grant from the
666 Doctoral School « Sciences du Végétal », Université Paris-Saclay.

667

668 **Availability of data and materials**

669 The genomic raw data were deposited into the NCBI SRA under the accessions PRJNA752967 for Sl3
670 and PRJNA752962 for Vv3. Genome assemblies were deposited at NCBI under the accessions
671 CP080979-CP080996 for Sl3 and CP080961-CP080978 for Vv3. Small RNAs raw data and the matrix of
672 sequence counts were deposited into the NCBI GEO under accession GSE181592. Furthermore, the
673 genomic and annotation (gene/TE) fasta and gff files, as well as Sl3 and Vv3 genome browsers are
674 available at the INRAE BIOGER Bioinformatics platform (https://bioinfo.bioger.inrae.fr/).

675 **Conflict of interest disclosure**

676 The authors declare they have no conflict of interest relating to the content of this article.

677

678

679 **References**

680

681 Amselem, J., Cuomo, C. A., van Kan, J. A. L., Viaud, M., Benito, E. P., Couloux, A., Coutinho, P. M., de
682 Vries, R. P., Dyer, P. S., Fillinger, S., Fournier, E., Gout, L., Hahn, M., Kohn, L., Lapalu, N.,
683 Plummer, K. M., Pradier, J. M., Quévillon, E., Sharon, A., … Dickman, M. (2011). Genomic
684 analysis of the necrotrophic fungal pathogens sclerotinia sclerotiorum and botrytis cinerea.
685 *PLoS Genetics*, *7*(8). https://doi.org/10.1371/journal.pgen.1002230

686 Amselem, J., Lebrun, M. H., & Quesneville, H. (2015). Whole genome comparative analysis of
687 transposable elements provides new insight into mechanisms of their inactivation in fungal
688 genomes. *BMC Genomics*, *16*(1). https://doi.org/10.1186/s12864-015-1347-1

689 Atwell, S., Corwin, J. A., Soltis, N. E., Subedy, A., Denby, K. J., & Kliebenstein, D. J. (2015). Whole
690 genome resequencing of Botrytis cinerea isolates identifies high levels of standing diversity.
691 *Frontiers in Microbiology*, *6*(SEP). https://doi.org/10.3389/FMICB.2015.00996

692 Bertazzoni, S., Williams, A. H., Jones, D. A., Syme, R. A., Tan, K.-C., & Hane, J. K. (2018). Accessories
693 Make the Outfit: Accessory Chromosomes and Other Dispensable DNA Regions in Plant-
694 Pathogenic Fungi. *Molecular Plant-Microbe Interactions®*, *31*(8), 779–788.
695 https://doi.org/10.1094/mpmi-06-17-0135-fi

696 Blanco-Ulate, B., Allen, G., Powell, A. L. T., & Cantu, D. (2013). Draft genome sequence of Botrytis
697 cinerea BcDW1, inoculum for noble rot of grape berries. *Genome Announcements*, *1*(3).
698 https://doi.org/10.1128/genomeA.00252-13

699 Castanera, R., Pérez, G., López, L., Sancho, R., Santoyo, F., Alfaro, M., Gabaldón, T., Pisabarro, A. G.,
700 Oguiza, J. A., & Ramírez, L. (2014). Highly expressed captured genes and cross-kingdom domains
701 present in Helitrons create novel diversity in pleurotus ostreatus and other fungi. *BMC*

Genomics, *15*(1). https://doi.org/10.1186/1471-2164-15-1071

Chellapan, B. V., Van Dam, P., Rep, M., Cornelissen, B. J. C., & Fokkens, L. (2016). Non-canonical Helitrons in Fusarium oxysporum. *Mobile DNA*, *7*(1). https://doi.org/10.1186/S13100-016-0083-7

Choquer, M., Fournier, E., Kunz, C., Levis, C., Pradier, J. M., Simon, A., & Viaud, M. (2007). Botrytis cinerea virulence factors: New insights into a necrotrophic and polyphageous pathogen. In *FEMS Microbiology Letters* (Vol. 277, Issue 1, pp. 1–10). FEMS Microbiol Lett. https://doi.org/10.1111/j.1574-6968.2007.00930.x

Derbyshire, M., Denton-Giles, M., Hegedus, D., Seifbarghi, S., Rollins, J., Kan, J. Van, Seidl, M. F., Faino, L., Mbengue, M., Navaud, O., Raffaele, S., Hammond-Kosack, K., Heard, S., & Oliver, R. (2017). The complete genome sequence of the phytopathogenic fungus Sclerotinia sclerotiorum reveals insights into the genome architecture of broad host range pathogens. *Genome Biology and Evolution*, *9*(3), 593–618. https://doi.org/10.1093/gbe/evx030

Diolez, A., Marches, F., Fortini, D., & Brygoo, Y. (1995). Boty, a long-terminal-repeat retroelement in the phytopathogenic fungus Botrytis cinerea. *Applied and Environmental Microbiology*, *61*(1), 103–108. https://doi.org/10.1128/AEM.61.1.103-108.1995

Drillon, G., Carbone, A., & Fischer, G. (2014). SynChro: A fast and easy tool to reconstruct and visualize synteny blocks along eukaryotic chromosomes. *PLoS ONE*, *9*(3). https://doi.org/10.1371/journal.pone.0092621

Elad, Y., Vivier, M., & Fillinger, S. (2015). Botrytis, the good, the bad and the ugly. In *Botrytis - The Fungus, the Pathogen and its Management in Agricultural Systems* (pp. 1–15). Springer International Publishing. https://doi.org/10.1007/978-3-319-23371-0_1

Flutre, T., Duprat, E., Feuillet, C., & Quesneville, H. (2011). Considering transposable element

725 diversification in de novo annotation approaches. *PLoS ONE*, *6*(1).
726 https://doi.org/10.1371/journal.pone.0016526

727 Fouché, S., Oggenfuss, U., Chanclud, E., & Croll, D. (2021). A devil's bargain with transposable
728 elements in plant pathogens. *Trends in Genetics : TIG*, *38*(3), 222–230.
729 https://doi.org/10.1016/J.TIG.2021.08.005

730 Gao, W., Khang, C. H., Park, S. Y., Lee, Y. H., & Kang, S. (2002). Evolution and organization of a highly
731 dynamic, subtelomeric helicase gene family in the rice blast fungus Magnaporthe grisea.
732 *Genetics*, *162*(1), 103–112. https://doi.org/10.1093/genetics/162.1.103

733 Geib, E., Gressler, M., Viediernikova, I., Hillmann, F., Jacobsen, I. D., Nietzsche, S., Hertweck, C., &
734 Brock, M. (2016). A Non-canonical Melanin Biosynthesis Pathway Protects Aspergillus terreus
735 Conidia from Environmental Stress. *Cell Chemical Biology*, *23*(5), 587–597.
736 https://doi.org/10.1016/j.chembiol.2016.03.014

737 Gilchrist, C. L. M., & Chooi, Y.-H. (2021). clinker & clustermap.js: automatic generation of gene cluster
738 comparison figures. *Bioinformatics*, *37*(16), 2473–2475.
739 https://doi.org/10.1093/bioinformatics/btab007

740 Gladieux, P., Condon, B., Ravel, S., Soanes, D., Maciel, J. L. N., Nhani, A., Chen, L., Terauchi, R.,
741 Lebrun, M. H., Tharreau, D., Mitchell, T., Pedley, K. F., Valent, B., Talbot, N. J., Farman, M., &
742 Fournier, E. (2018). Gene Flow between Divergent Cereal- and Grass-Specific Lineages of the
743 Rice Blast Fungus Magnaporthe oryzae. *MBio*, *9*(1). https://doi.org/10.1128/MBIO.01219-17

744 Gurevich, A., Saveliev, V., Vyahhi, N., & Tesler, G. (2013). QUAST: Quality assessment tool for genome
745 assemblies. *Bioinformatics*, *29*(8), 1072–1075. https://doi.org/10.1093/bioinformatics/btt086

746 Hoede, C., Arnoux, S., Moisset, M., Chaumier, T., Inizan, O., Jamilloux, V., & Quesneville, H. (2014).
747 PASTEC: An automatic transposable element classification tool. *PLoS ONE*, *9*(5).

https://doi.org/10.1371/journal.pone.0091929

Kjærbølling, I., Vesth, T., Frisvad, J. C., Nybo, J. L., Theobald, S., Kildgaard, S., Petersen, T. I., Kuo, A., Sato, A., Lyhne, E. K., Kogle, M. E., Wiebenga, A., Kun, R. S., Lubbers, R. J. M., Mäkelä, M. R., Barry, K., Chovatia, M., Clum, A., Daum, C., … Andersen, M. R. (2020). A comparative genomics study of 23 Aspergillus species from section Flavi. *Nature Communications*, *11*(1). https://doi.org/10.1038/s41467-019-14051-y

Kojima, K. K. (2019). Structural and sequence diversity of eukaryotic transposable elements. *Genes and Genetic Systems*, *94*(6), 233–252. https://doi.org/10.1266/ggs.18-00024

Koren, S., Walenz, B. P., Berlin, K., Miller, J. R., Bergman, N. H., & Phillippy, A. M. (2017). Canu: Scalable and accurate long-read assembly via adaptive κ-mer weighting and repeat separation. *Genome Research*, *27*(5), 722–736. https://doi.org/10.1101/gr.215087.116

Levis, C., Giraud, T., Dutertre, M., Fortini, D., & Brygoo, Y. (1997a). Telomeric DNA of Botrytis cinerea: a useful tool for strain identification. *FEMS Microbiology Letters*, *157*(2), 267–272. https://doi.org/10.1111/J.1574-6968.1997.TB12783.X

Levis, C., Fortini, D., & Brygoo, Y. (1997b). Flipper, a mobile Fot1-like transposable element in Botrytis cinerea. *Molecular and General Genetics*, *254*(6), 674–680. https://doi.org/10.1007/s004380050465

Lind, A. L., Wisecaver, J. H., Lameiras, C., Wiemann, P., Palmer, J. M., Keller, N. P., Rodrigues, F., Goldman, G. H., & Rokas, A. (2017). Drivers of genetic diversity in secondary metabolic gene clusters within a fungal species. *PLoS Biology*, *15*(11). https://doi.org/10.1371/JOURNAL.PBIO.2003583

Lombard, V., Golaconda Ramulu, H., Drula, E., Coutinho, P. M., & Henrissat, B. (2014). The carbohydrate-active enzymes database (CAZy) in 2013. *Nucleic Acids Research*, *42*(D1).

https://doi.org/10.1093/nar/gkt1178

Martin, M. (2011). TECHNICAL NOTES. In *EMBnet.journal* (Vol. 17, Issue 1). http://www-huber.embl.de/users/an-

Mbengue, M., Navaud, O., Peyraud, R., Barascud, M., Badet, T., Vincent, R., Barbacci, A., & Raffaele, S. (2016). Emerging trends in molecular interactions between plants and the broad host range fungal pathogens botrytis cinerea and sclerotinia sclerotiorum. In *Frontiers in Plant Science* (Vol. 7, Issue MAR2016). Frontiers Media S.A. https://doi.org/10.3389/fpls.2016.00422

Meena, M., Gupta, S. K., Swapnil, P., Zehra, A., Dubey, M. K., & Upadhyay, R. S. (2017). Alternaria toxins: Potential virulence factors and genes related to pathogenesis. In *Frontiers in Microbiology* (Vol. 8, Issue AUG). Frontiers Media S.A. https://doi.org/10.3389/fmicb.2017.01451

Mercier, A., Carpentier, F., Duplaix, C., Auger, A., Pradier, J. M., Viaud, M., Gladieux, P., & Walker, A. S. (2019). The polyphagous plant pathogenic fungus Botrytis cinerea encompasses host-specialized and generalist populations. *Environmental Microbiology*, *21*(12), 4808–4821. https://doi.org/10.1111/1462-2920.14829

Mercier, A., Simon, A., Lapalu, N., Giraud, T., Bardin, M., Walker, A.S., Viaud, M., & Gladieux, P. (2021). Population genomics reveals molecular determinants of specialization to tomato in the polyphagous fungal pathogen Botrytis cinerea in France. *Phytopathology®*. https://doi.org/10.1094/phyto-07-20-0302-fi

Olarte, R. A., Menke, J., Zhang, Y., Sullivan, S., Slot, J. C., Huang, Y., Badalamenti, J. P., Quandt, A. C., Spatafora, J. W., & Bushley, K. E. (2019). Chromosome rearrangements shape the diversification of secondary metabolism in the cyclosporin producing fungus Tolypocladium inflatum. *BMC Genomics*, *20*(1). https://doi.org/10.1186/s12864-018-5399-x

794 Plesken, C., Pattar, P., Reiss, B., Noor, Z. N., Zhang, L., Klug, K., Huettel, B., & Hahn, M. (2021). Genetic
795 Diversity of Botrytis cinerea Revealed by Multilocus Sequencing, and Identification of B. cinerea
796 Populations Showing Genetic Isolation and Distinct Host Adaptation. *Frontiers in Plant Science*,
797 *12*. https://doi.org/10.3389/fpls.2021.663027

798 Porquier, A., Moraga, J., Morgant, G., Dalmais, B., Simon, A., Sghyer, H., Collado, I. G., & Viaud, M.
799 (2019). Botcinic acid biosynthesis in Botrytis cinerea relies on a subtelomeric gene cluster
800 surrounded by relics of transposons and is regulated by the Zn2Cys6 transcription factor
801 BcBoa13. *Current Genetics*, *65*(4), 965–980. https://doi.org/10.1007/s00294-019-00952-4

802 Porquier, A., Morgant, G., Moraga, J., Dalmais, B., Luyten, I., Simon, A., Pradier, J. M., Amselem, J.,
803 Collado, I. G., & Viaud, M. (2016). The botrydial biosynthetic gene cluster of Botrytis cinerea
804 displays a bipartite genomic structure and is positively regulated by the putative Zn(II)2Cys6
805 transcription factor BcBot6. *Fungal Genetics and Biology*, *96*, 33–46.
806 https://doi.org/10.1016/j.fgb.2016.10.003

807 Porquier, A., Tisserant, C., Salinas, F., Glassl, C., Wange, L., Enard, W., Hauser, A., Hahn, M., &
808 Weiberg, A. (2021). Retrotransposons as pathogenicity factors of the plant pathogenic fungus
809 Botrytis cinerea. *Genome Biology*, *22*(1). https://doi.org/10.1186/s13059-021-02446-4

810 Quesneville, H., Bergman, C. M., Andrieu, O., Autard, D., Nouaud, D., Ashburner, M., & Anxolabehere,
811 D. (2005). Combined evidence annotation of transposable elements in genome sequences. *PLoS*
812 *Computational Biology*, *1*(2), 0166–0175. https://doi.org/10.1371/journal.pcbi.0010022

813 Rehmeyer, C. J., Li, W., Kusaba, M., & Farman, M. L. (2009). The telomere-linked helicase (TLH) gene
814 family in Magnaporthe oryzae: Revised gene structure reveals a novel TLH-specific protein
815 motif. In *Current Genetics* (Vol. 55, Issue 3, pp. 253–262). Curr Genet.
816 https://doi.org/10.1007/s00294-009-0240-3

817 Sánchez-Alonso, P., & Guzmán, P. (1998). Organization of chromosome ends in Ustilago maydis.

818 RecQ-like helicase motifs at telomeric regions. *Genetics*, *148*(3), 1043–1054.
819 https://doi.org/10.1093/genetics/148.3.1043

820 Shumate, A., & Salzberg, S. L. (2021). Liftoff: accurate mapping of gene annotations. *Bioinformatics*,
821 *37*(12), 1639–1643. https://doi.org/10.1093/bioinformatics/btaa1016

822 Simon, A., Dalmais, B., Morgant, G., & Viaud, M. (2013). Screening of a Botrytis cinerea one-hybrid
823 library reveals a Cys2His2 transcription factor involved in the regulation of secondary
824 metabolism gene clusters. *Fungal Genetics and Biology*, *52*, 9–19.
825 https://doi.org/10.1016/j.fgb.2013.01.006

826 Solovyev, V., Kosarev, P., Seledsov, I., & Vorobyev, D. (2006). Automatic annotation of eukaryotic
827 genes, pseudogenes and promoters. *Genome Biology*, *7 Suppl 1*(Suppl 1).
828 https://doi.org/10.1186/gb-2006-7-s1-s10

829 Stukenbrock, E. H., & McDonald, B. A. (2008). The Origins of Plant Pathogens in Agro-Ecosystems.
830 *Http://Dx.Doi.Org/10.1146/Annurev.Phyto.010708.154114*, *46*, 75–100.
831 https://doi.org/10.1146/ANNUREV.PHYTO.010708.154114

832 Tolios, A., Teupser, D., & Holdt, L. M. (2015). Preanalytical conditions and DNA isolation methods
833 affect telomere length quantification in whole blood. *PLoS ONE*, *10*(12).
834 https://doi.org/10.1371/journal.pone.0143889

835 Valero-Jiménez, C. A., Steentjes, M. B. F., Slot, J. C., Shi-Kunne, X., Scholten, O. E., & van Kan, J. A. L.
836 (2020). Dynamics in secondary metabolite gene clusters in otherwise highly syntenic and stable
837 genomes in the fungal genus botrytis. *Genome Biology and Evolution*, *12*(12), 2491–2507.
838 https://doi.org/10.1093/GBE/EVAA218

839 van Kan, J.A.L., Goverse, A. & Van Der Vlugt-Bergmans, C.J.B. Electrophoretic karyotype analysis of
840 Botrytis cinerea. *Neth. J. Pl. Path.* **99** (Suppl 3), 119–128 (1993).

https://doi.org/10.1007/BF03041402

van Kan, J. A. L., Stassen, J. H. M., Mosbach, A., Van Der Lee, T. A. J., Faino, L., Farmer, A. D., Papasotiriou, D. G., Zhou, S., Seidl, M. F., Cottam, E., Edel, D., Hahn, M., Schwartz, D. C., Dietrich, R. A., Widdison, S., & Scalliet, G. (2017). A gapless genome sequence of the fungus Botrytis cinerea. *Molecular Plant Pathology*, *18*(1), 75–89. https://doi.org/10.1111/mpp.12384

Veloso, J., & van Kan, J. A. L. (2018). Many Shades of Grey in Botrytis–Host Plant Interactions. In *Trends in Plant Science* (Vol. 23, Issue 7, pp. 613–622). Elsevier Ltd. https://doi.org/10.1016/j.tplants.2018.03.016

Vigneault, F., Ter-Ovanesyan, D., Alon, S., Eminaga, S., Christodoulou, D. C., Seidman, J. G., Eisenberg, E., & Church, G. M. (2012). High-throughput multiplex sequencing of miRNA. *Current Protocols in Human Genetics*, *Chapter 11*(SUPPL.73). https://doi.org/10.1002/0471142905.hg1112s73

Walker, A. S. (2015). Diversity within and between species of Botrytis. In *Botrytis - The Fungus, the Pathogen and its Management in Agricultural Systems* (pp. 91–125). Springer International Publishing. https://doi.org/10.1007/978-3-319-23371-0_6

Walker, A. S., Gladieux, P., Decognet, V., Fermaud, M., Confais, J., Roudet, J., Bardin, M., Bout, A., C. Nicot, P., Poncet, C., & Fournier, E. (2015). Population structure and temporal maintenance of the multihost fungal pathogen Botrytis cinerea: Causes and implications for disease management. *Environmental Microbiology*, *17*(4), 1261–1274. https://doi.org/10.1111/1462-2920.12563

Walker, B. J., Abeel, T., Shea, T., Priest, M., Abouelliel, A., Sakthikumar, S., Cuomo, C. A., Zeng, Q., Wortman, J., Young, S. K., & Earl, A. M. (2014). Pilon: An integrated tool for comprehensive microbial variant detection and genome assembly improvement. *PLoS ONE*, *9*(11). https://doi.org/10.1371/journal.pone.0112963

Weiberg, A., Wang, M., Lin, F. M., Zhao, H., Zhang, Z., Kaloshian, I., Huang, H. Da, & Jin, H. (2013). Fungal small RNAs suppress plant immunity by hijacking host RNA interference pathways. *Science*, *342*(6154), 118–123. https://doi.org/10.1126/science.1239705

Wicker, T., Sabot, F., Hua-Van, A., Bennetzen, J. L., Capy, P., Chalhoub, B., Flavell, A., Leroy, P., Morgante, M., Panaud, O., Paux, E., SanMiguel, P., & Schulman, A. H. (2007). A unified classification system for eukaryotic transposable elements. In *Nature Reviews Genetics* (Vol. 8, Issue 12, pp. 973–982). Nature Publishing Group. https://doi.org/10.1038/nrg2165

Yang, H., Yu, H., & Ma, L. J. (2020). Accessory chromosomes in fusarium oxysporum. In *Phytopathology* (Vol. 110, Issue 9, pp. 1488–1496). American Phytopathological Society. https://doi.org/10.1094/PHYTO-03-20-0069-IA

876 ## Supplemental information:

877 **File S1**: Consensus sequences of the repeated elements identified in the genomes of *B. cinerea* strains
878 Sl3 and Vv3.

879 **Table S1:** Chromosomes of the *B. cinerea* strains B05.10, Sl3 and Vv3.

880 **Table S2:** Genes predicted in the genomes of *B. cinerea* strains B05.10, Sl3 and Vv3.

881 **Table S3**: Repertoires of Transposable Elements (TEs) in the *B. cinerea* strains B05.10, Sl3 and Vv3.

882 **Table S4**: Libraries of small RNAs isolated from *B. cinerea* strains belonging to different populations.

883 **Table S5:** List of PCR primers used to detect the presence of Transposable Elements (TEs) or the gene
884 encoding the Telomere-Linked Telomerase (*BcTLH*).

885

886 **Figure S1:** Genomic genealogy of *B. cinerea* strains showing the populations T, G1 and G2.

887 **Figure S2:** CHEF gel electrophoresis resolving accessory chromosomes of *B. cinerea* strains B05.10, Sl3
888 and Vv3.

889 **Figure S3:** Synteny between the Core Chromosomes (CCs) of the *B. cinerea* strains B05.10, Sl3 and Vv3.

890 **Figure S4**: Main inversions events observed between the genomes of the *B. cinerea* strains Sl3 and Vv3.

891 **Figure S5:** Localization of the PKS7 secondary metabolism gene cluster in the genomes of the *B. cinerea*
892 strains B05.10 and Vv3.

893 **Figure S6**: Duplication of four contiguous genes in the genome of the *B. cinerea* strain Sl3.

894 **Figure S7:** Structure of the Telomere-Linked Helicase (TLH) identified in the *B. cinerea* strain Vv3.

895 **Figure S8:** Positions of the genes encoding the Telomere-Linked Helicase (BcTLH) and of the Helitron-
896 like Transposable Elements (TE) in the genome of the *B. cinerea* strain Vv3.

897 **Figure S9:** Alignment of the ten consensus sequences corresponding to the *Boty*/Gypsy_1
898 Transposable Element (TE) identified in the genomes of the *B. cinerea* strains B05.10, Sl3 or Vv3.

899 **Figure S10:** Helitron-like Transposable Element (TE) identified in the genome of the *B. cinerea* strain
900 Vv3.

901 **Figure S11:** Localization of the main superfamilies of Transposable Elements (TEs) in the genomes of
902 the *B. cinerea* strains Sl3 and Vv3.

903 **Figure S12:** GC content of complete copies of the main subfamilies of Transposable Elements (TEs) in
904 the genomes of the *B. cinerea* strains B05.10, Sl3 and Vv3.

905 **Figure S13:** Principal Component Analysis (PCA) of the repertoires of small RNAs in different strains of
906 *B. cinerea*.

907 **Figure S14:** Retrotransposons that generate small RNAs in the *B. cinerea* strains Sl3 and/or Vv3.

908 **Figure S15:** Mapping of small RNA reads on complete copies of TEs in relation to their GC percent.

909 **Figure S16:** Small RNAs produced by the *B. cinerea* strains Sl3 and Vv3: size distribution and 5'
910 nucleotide.

911 **Figure S17:** Positions of complete copies of the TE Copia_4, Gypsy_6 and Gypsy_7 in the *B. cinerea* Vv3
912 genome.

913 **Figure S18:** Alignment of Copia_4, Gypsy_6 and Gypsy_7 consensus sequences with their respective
914 complete copies in Vv3 genome.

Figures & Tables

Table 1: **Distribution of Accessory Chromosomes (ACs) and a selection of dispensable genes and Transposable Elements (TEs) in *B. cinerea* strains from different populations.** The genomic features highlighted in the present study, using complete assemblies of Sl3 and Vv3 genomes, were investigated in populations specialized either on grapevine (G1 and G2) either on tomato (T; Mercier et al., 2021). The distribution of ACs and secondary metabolism key genes were investigated using Illumina genomic data (Mercier et al., 2021) while those of the TEs and of the gene encoding the telomere-linked helicase (BcHTL) were investigated by PCR. a. van Kan et al., 2017. b. Mercier et al., 2021. c. Amselem et al., 2011. d. Blanco-Ulate et al., 2013. Nd, not determined. ✔, presence. -, absence. (✔), partial presence of an AC. Nd, Not determined.

Population	Strain	Host	Location	Ref	Accessory chromosomes (Illumina sequencing; Ref b)			Presence of gene (Illumina sequencing; Ref b)			Presence of TE or gene (PCR detection)				
					AC 17	AC 18	AC 19	*Bcstc6*	*BcmelA*	*Bcdtc*	*Bctlh*	Helitron-like	Copia_4	Gypsy_6	Gypsy_7
Nd	B05.10	unknown	unknown	a	✔	✔	-	-	✔	-	-	-	-	-	-
T	Sl1	*Solanum lycopersicum*	Bourgogne	b	✔	-	-	-	-	✔	-	-	-	-	-
	Sl2		Champagne	b	✔	-	-	-	-	✔	-	-	-	-	-
	Sl3		Champagne	b	✔	(✔)	-	✔	-	✔	-	-	-	-	-
	Sl4		Provence	b	✔	-	-	-	-	✔	-	-	-	-	-
	Sl5		Provence	b	✔	✔	-	-	-	✔	✔	-	-	-	-
	Sl6		Rhône-Alpes	b	✔	-	-	-	-	-	-	-	-	-	-
	Sl7		Rhône-Alpes	b	✔	-	-	-	-	✔	-	-	-	-	-
	Sl8		Rhône-Alpes	b	✔	-	-	-	-	-	-	-	-	-	-
	Sl9		Occitanie	b	-	✔	-	-	-	✔	-	-	-	-	-
	Sl10		Occitanie	b	-	-	-	-	-	✔	-	✔	-	-	-
	Sl11		Occitanie	b	✔	-	-	-	-	-	✔	-	-	-	-
	Sl12		Occitanie	b	✔	-	-	-	-	-	✔	-	-	-	-
	Sl13		Occitanie	b	✔	-	-	✔	-	✔	✔	-	-	-	-
G1	Vv1	*Vitis vinifera*	Champagne	b	✔	-	✔	✔	✔	✔	✔	✔	✔	-	✔
	Vv2		Champagne	b	✔	-	✔	✔	✔	✔	✔	✔	✔	-	-
	Vv3		Champagne	b	✔	-	✔	-	✔	✔	✔	✔	✔	✔	✔
	Vv4		Champagne	b	✔	-	✔	-	✔	✔	✔	✔	✔	-	✔
	Vv5		Champagne	b	✔	-	✔	✔	✔	✔	✔	✔	✔	-	✔
	Vv6		Champagne	b	✔	-	✔	-	✔	✔	-	✔	✔	-	✔
	Vv7		Provence	b	✔	-	✔	-	✔	✔	-	✔	✔	-	✔
	Vv10		Provence	b	✔	-	✔	✔	✔	✔	✔	✔	✔	✔	✔
	Vv12		Provence	b	✔	-	✔	✔	✔	✔	✔	✔	✔	-	✔
	Vv13		Provence	b	✔	-	-	-	✔	✔	✔	✔	✔	✔	✔
	Vv14		Provence	b	✔	-	✔	-	✔	✔	✔	✔	✔	-	✔
	Vv16		Champagne	b	✔	-	✔	✔	✔	✔	✔	✔	✔	-	✔
G2	Vv8	*Vitis vinifera*	Provence	b	✔	-	-	-	✔	✔	✔	✔	-	-	✔
	Vv9		Provence	b	✔	✔	-	-	✔	✔	✔	-	-	-	-
	Vv11		Provence	b	✔	✔	-	-	✔	-	✔	-	-	-	-
	Vv15		Provence	b	-	-	-	✔	✔	✔	-	✔	-	-	-
Nd	Rf1	*Rubus fruticosus*	Bourgogne	b	✔	-	-	✔	✔	-	-	-	-	✔	-
Nd	Rf2	*Rubus fruticosus*	Champagne	b	(✔)	-	-	-	-	-	✔	✔	✔	✔	✔
Nd	Hm1	*Hydrangea macrophylla*	Anjou	b	✔	✔	-	-	✔	-	-	-	-	✔	-
Nd	T4	*Solanum lycopersicum*	Provence	c	-	-	-	✔	-	-	-	-	-	-	-
Nd	BcDW1	*Vitis vinifera*	California	d	✔	✔	-	✔	✔	✔	Nd	Nd	Nd	Nd	Nd

A.

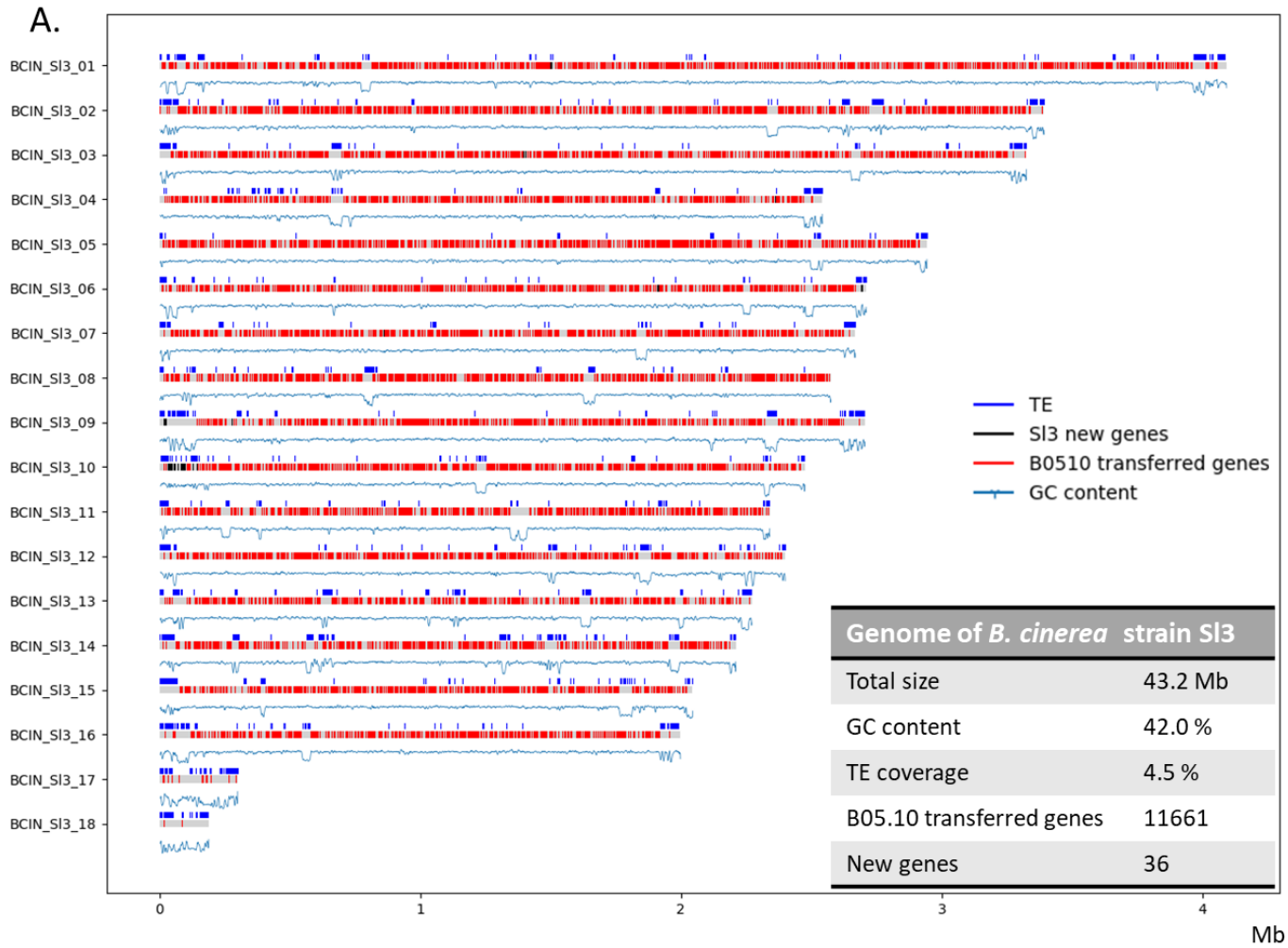

Genome of *B. cinerea* strain Sl3	
Total size	43.2 Mb
GC content	42.0 %
TE coverage	4.5 %
B05.10 transferred genes	11661
New genes	36

927

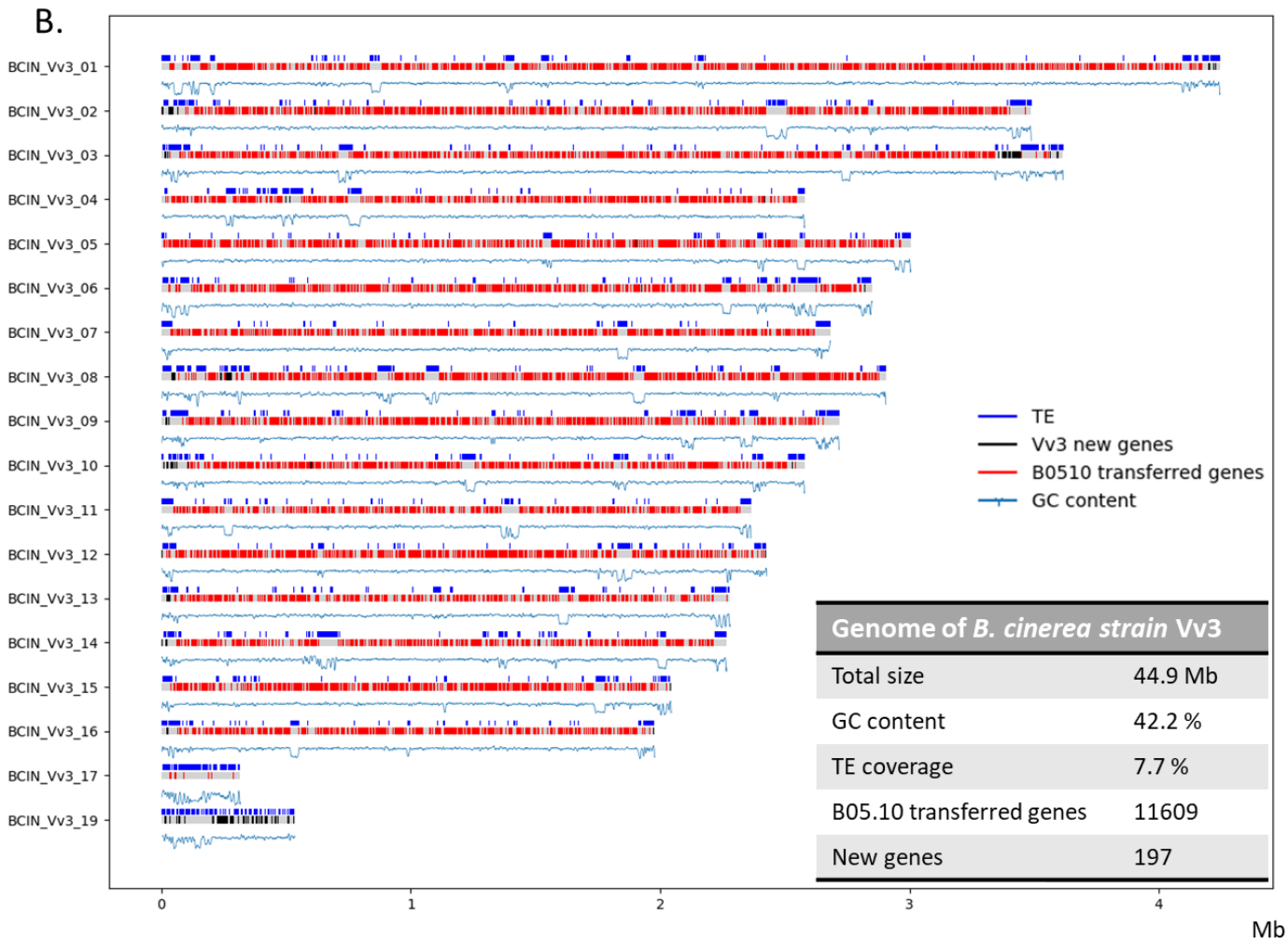

Genome of *B. cinerea strain* Vv3	
Total size	44.9 Mb
GC content	42.2 %
TE coverage	7.7 %
B05.10 transferred genes	11609
New genes	197

Figure 1: Genome organization in *B. cinerea* strains Sl3 (A) and Vv3 (B). The two karyoplots show the 18 chromosomes identified in each strain, genes previously predicted in the B05.10 reference strain (van Kan et al., 2017; red), newly detected genes (black), Transposable Elements (TEs; dark blue) and the GC content (blue) along the Core Chromosomes (CCs BCIN_01 to 16) and the Accessory Chromosomes (ACs BCIN_17 to 19).

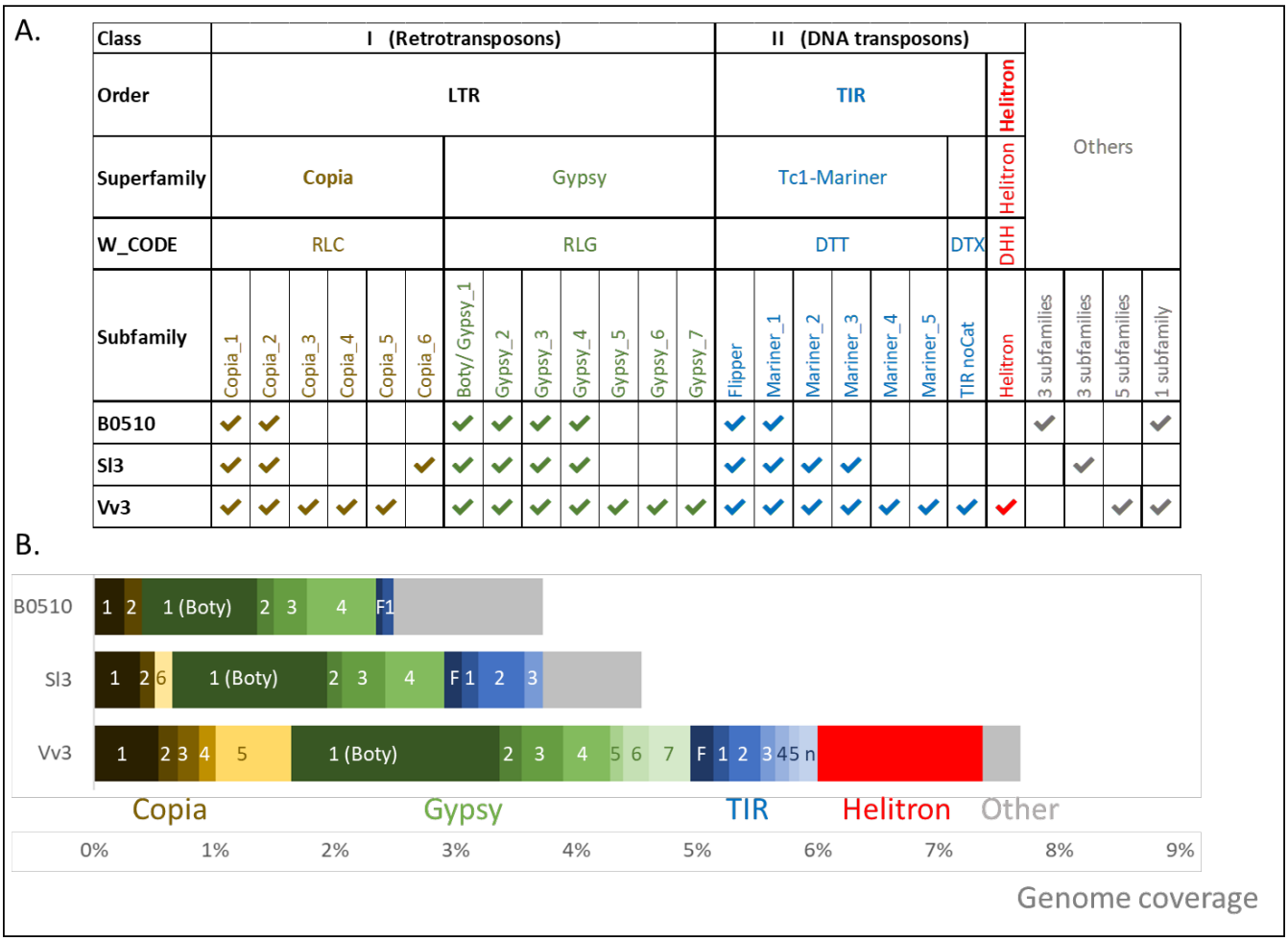

Figure 2: Transposable Elements (TEs) in the genomes of the *B. cinerea* strains B05.10, Sl3 and Vv3. **A**. Subfamilies of TEs identified in the Sl3 and Vv3 strains were classified according to Wicker et al., (2007), as previously done for the strain B05.10 (Porquier et al., 2016). In the present study, all *Boty* consensus were merged into a single subfamily. **B.** Total genome coverage was detailed for the different subfamilies. For more details, see Sup. Table 3.

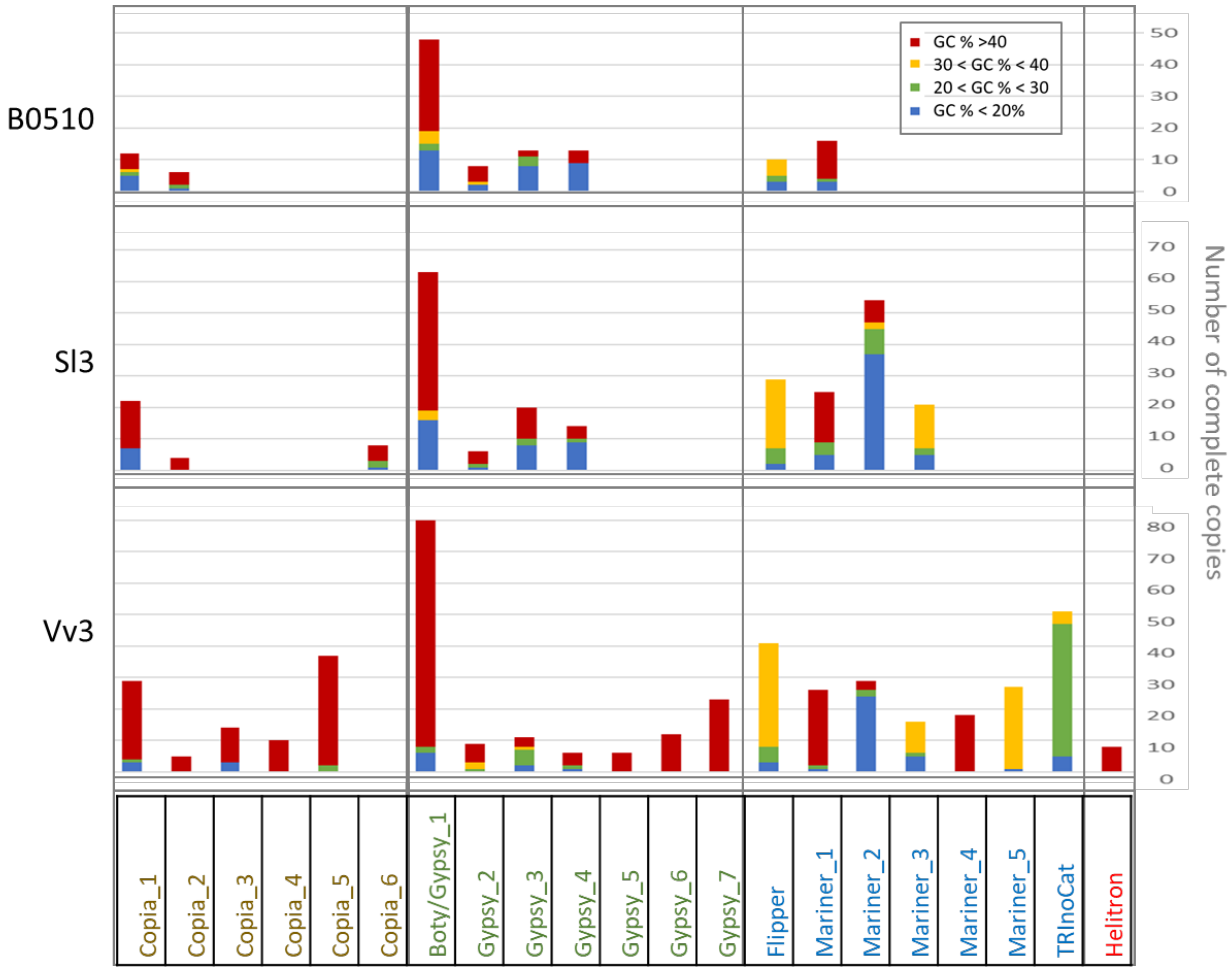

Figure 3: GC content of complete copies of the main Transposable Elements (TEs) in the genomes of *B. cinerea* strains B05.10, Sl3 and Vv3. The complete copies of each subfamily of TEs were classified according to their GC content. See Sup. Fig. S11 for more details.

Table 2: Small RNAs produced by the Transposable Elements (TEs) identified in the *B. cinerea* strains B05.10, SI3 and Vv3. Small RNA libraries were made from strains cultivated on grape juice medium except two that were done from strains cultivated on tomato juice medium (indicated by -T*). Reads from the 16 libraries were mapped on the TEs to identify the small RNA-producing retrotransposons. For small RNAs, ✔ indicates that at least 300 Reads Per Million (RPMs) from the library are mapping on the corresponding TE. Genomes in which the TEs were identified are reminded at the top of the table (✔, presence. -, absence). For more details, see Sup. Table S4.

Subfamily name			Copia_1	Copia_2	Copia_3	Copia_4	Copia_5	Copia_6	Boty_ Gypsy_1	Gypsy_2	Gypsy_3	Gypsy_4	Gypsy_5	Gypsy_6	Gypsy_7
Genomes in which the TE was identified		B0510	✔	✔	-	-	-	-	✔	✔	✔	✔	-	-	-
		SI3	✔	✔	-	-	-	✔	✔	✔	✔	✔	-	-	-
		Vv3	✔	✔	✔	✔	✔	-	✔	✔	✔	✔	✔	✔	✔
Libraries of small RNAs		B0510							✔		✔	✔			
	T population	SI1							✔		✔				
		SI2							✔		✔	✔			
		SI3						✔	✔		✔	✔			
		SI3-T*						✔	✔		✔	✔			
		SI6	✔					✔	✔		✔	✔			
		SI11							✔			✔			
		SI13							✔		✔	✔			
	G1 population	Vv1				✔			✔		✔	✔		✔	✔
		Vv3				✔			✔		✔	✔		✔	✔
		Vv3-T*				✔			✔		✔	✔		✔	✔
		Vv5				✔			✔		✔	✔		✔	✔
		Vv14				✔			✔		✔	✔		✔	✔
	G2 population	Vv8							✔			✔			
		Vv9													
		Vv15							✔			✔			